

Dual-, Ternary- and $(\Delta + 1)$ -Unitaries

A path to exact solutions of dynamics for
multidimensional quantum lattices

Richard Maximilian Milbradt

Advisor & 1st Referee: Prof. Christian Mendl
2nd Referee: Prof. Jan von Delft

A thesis presented for the degree of
Master of Science



Theoretical and Mathematical Physics
Technische Universität München &
Ludwig-Maximilians-Universität München
Germany

November 25, 2021

Declaration of Authorship

I hereby certify that this thesis is my own original work. All results and thoughts not made by myself are referenced. All figures have been created by myself.

Acknowledgements

First of all I want to thank my supervisor Prof. Christian Mendl, who consistently provided guidance and help as well as the initial starting point for this thesis. Next is Prof. Jan von Delft, who not only kindly agreed to be the second referee for the thesis, but whose lecture on tensor networks provided inspiration and a good foundation of the topic. Without it this thesis would look quite different. Although not exactly providing input on this thesis, I want to thank Prof. Sabine Jansen. She did an excellent job as mentor and helped find my way in the TMP-program. Finally I need to thank friends and family, who provided encouragement and support during the last years. They helped to keep me lively during the Corona pandemic and at least metaphorically reduce the distance we were required to keep. Special thanks goes to Sarah Joswig who proofread this thesis in meticulous detail, which helped to improve understandability and spelling of the text.

Contents

1	Nomenclature	4
2	Introduction	5
3	Motivation via Trotterisation	6
4	Dual Unitary Operators	7
4.1	Visualisation and Definition	7
4.2	Correlation Functions in 1+1 Dimensions	12
5	Ternary Unitary Operators	19
5.1	The Set of Ternary Unitaries	19
5.2	Correlation Functions in 2+1 Dimensions	23
5.3	Other Time-Evolutions	31
6	Extension to an arbitrary Number of spatial Dimensions	35
6.1	Definition and Correlation Functions	35
6.2	Properties of the M-Map	41
6.3	Examples of the M-Map	43
6.3.1	(1+1)-dimensional Lattices	44
6.3.2	(2+1)-dimensional Lattices	44
7	Unitaries and Index Permutations	45
8	Implementation on a Quantum Computer	48
8.1	Solvable initial States	48
8.2	Time-Evolution of local Observables	51
8.3	Implementation using Unitary Gates	52
8.3.1	Simplification of a Tensor Network	53
8.3.2	Conversion to a Quantum Circuit	55
8.4	Solvable States for two spatial Dimensions	60
9	Final Discussion and Outlook	64

1 Nomenclature

- For an object A , $\text{End}(A)$ is the set of endomorphisms on A .
- Exclusive or

$$\mathbf{XOR} \quad \text{or} \quad \leftrightarrow$$

- Floor and ceiling functions

$$\lfloor x \rfloor = \max\{m \in \mathbb{Z} | m \leq x\}, \quad \lceil x \rceil = \min\{m \in \mathbb{Z} | m \geq x\}$$

- Infinity norm for a vector $\vec{x} = (x_1, \dots, x_n)$.

$$\|\vec{x}\|_\infty = \max_i |x_i|$$

- Intervall $I_a(b) = \{a, a+1, \dots, b-1, b\}$ for $a, b \in \mathbb{Z}$ and the basic arithmetic operations are defined by acting element-wise, e.g.

$$I_a(b)/2 = \left\{ \frac{a}{2}, \frac{a+1}{2}, \dots, \frac{b-1}{2}, \frac{b}{2} \right\}.$$

- Pauli matrices

$$\sigma^x = \begin{pmatrix} 0 & 1 \\ 1 & 0 \end{pmatrix}, \quad \sigma^y = \begin{pmatrix} 0 & -i \\ i & 0 \end{pmatrix}, \quad \sigma^z = \begin{pmatrix} 1 & 0 \\ 0 & -1 \end{pmatrix}$$

- Permutation $\pi \in \sigma(A)$ for a finite set $A = \{a_1, a_2, \dots, a_{n-1}, a_n\}$ and $\sigma(A)$ the permutation group on A

$$\pi = \begin{pmatrix} a_1 & a_2 & \dots & a_{n-1} & a_n \\ \pi(a_1) & \pi(a_2) & \dots & \pi(a_{n-1}) & \pi(a_n) \end{pmatrix}$$

- $(n+m)$ -dimensional space-time has n space dimensions and m time dimensions.
- The trace over a set of sites A written as Tr_A .
- Unit operator/Identity operator $\mathbb{1}$
- Visualisation of the partial trace over a subsystem

$$\text{Tr}_2 [U_{(1,2)}] = \begin{array}{c} | \\ \text{---} \\ | \end{array} \begin{array}{c} \text{---} \\ U \\ \text{---} \end{array} \begin{array}{c} | \\ \text{---} \\ | \end{array} = \begin{array}{c} | \\ \text{---} \\ | \end{array} \begin{array}{c} \text{---} \\ U \\ \text{---} \end{array} \begin{array}{c} | \\ \text{---} \\ | \end{array}$$

2 Introduction

The study of many-body quantum systems is an ongoing field of research [1–5]. However, for two or higher dimensional systems exact solutions are rare and numerical methods hit a so-called "exponential wall" [5]. In [1] a special class of operators, called dual unitary operators, was introduced in order to further the development of an ergodic theory for quantum many-body systems. The general setting can be motivated by using a Trotterisation procedure. This is done in detail in section 3 and will serve as a gentle start to our journey. The use of dual unitaries as a time-evolution leads to exactly solvable correlation functions. While this was proven in [1], we will show in section 4 a slight variation of the proof in order to develop some of the language and methods, while still in the easy to visualize case of $(1 + 1)$ -dimensional space-time. We are also going to discuss some general properties of dual unitaries and give a proper definition. In section 5 we will make the jump to $(2 + 1)$ -dimensional space-time. We will introduce ternary unitary operators that are a canonical extension of the dual unitary operators. A definition and basic properties will be discussed and finally we are going to see the computation of exact correlation functions for ternary unitaries. In this section still, we will walk back a little and think about what exactly leads to these exact solutions by exploring different choices of time-evolutions for $(2 + 1)$ -dimensional space-time.

Equipped with this knowledge we can continue further. We will generalize the concept and proof to an arbitrary number of spatial dimensions, leading to the definition of $(\Delta + 1)$ -unitary operators in section 6. In all three sections we found some operator valued linear maps M_y . They are discussed in more detail in [1]. However, that discussion will be postponed until section 6, since it is very abstract even for $(1 + 1)$ -dimensional space-time and fairly easy to generalise. In section 7 we explore a little side-route. It will be even more abstract by analysing the concept behind the different kinds of unitary definitions. To this extend we make the index splitting of tensors more precise. We find further extensions and supersets of our $(\Delta + 1)$ -unitaries that are already analysed in the literature and have surprising applications in other fields.

In section 8, the final section introducing new content, we come back from the very abstract analysis to $(1 + 1)$ -dimensional space-time. Why do we do this? A potential way to avoid the exponential wall is to use quantum computers, for example by computing tensor networks diagrams. However, the tensor networks in the previous section include a lot of traces, some of them over time. [6] provides the concept of solvable states, which allow us to still obtain exact solutions for certain physical quantities. At the same time, it gets rid of most of the difficult to realise traces. This allows us to convert a tensor network diagram into a quantum circuit consisting of unitary gates. Since we know the exact solutions, we could use these quantum circuits to check the accuracy of our quantum computers, i.e. we can use it as a benchmark. So we will end the journey with a concrete application of the explored concept of dual and ternary unitaries.

3 Motivation via Trotterisation

While one could simply define dual unitary operators, one can also motivate them more thoroughly. Doing so makes the physical interpretation easier. We can start this motivation with one of the basic characteristics of quantum mechanics. It states that the time-evolution of a quantum mechanical system can be described using a Hamiltonian H , which is a hermitian operator. Assuming H does not depend on time, we may describe the time-evolution explicitly via

$$\mathbb{U}(t) = e^{-iHt}, \quad (1)$$

where the starting time is assumed to be $t_0 = 0$ [7] and natural units are used. Assume the Hamiltonian is of the form

$$H = \sum_j H_j, \quad (2)$$

where each H_j is a hermitian operator. We apply a Trotter-decomposition of first order to (1), i.e.

$$e^{-iHt} = \prod_j e^{-iH_j t} + \mathcal{O}(t^2). \quad (3)$$

The error occurs due to the possible non-commutativity of the H_j [8]. This decomposition is useful, as we want to examine systems made of smaller subsystems. To be more explicit assume a 1D-chain consisting of $2L$ subsystems. Each subsystem x will be in a state $|\psi_x\rangle \in \mathcal{H}_x$, where \mathcal{H}_x is a d -dimensional Hilbert space, e.g. \mathbb{C}^d . We will enumerate the different sites as follows:

$$x \quad \overset{\bullet}{0} \quad \overset{\bullet}{1} \quad \overset{\bullet}{2} \quad \overset{\bullet}{3} \quad \cdots \quad \overset{\bullet}{2L-2} \quad \overset{\bullet}{2L-1}. \quad (4)$$

Restricting ourselves to nearest-neighbour interactions, the Hamiltonian acting on the state of the complete system $|\Psi\rangle \in \mathcal{H} = \bigotimes_x \mathcal{H}_x$ becomes

$$H = \sum_{x=0}^{2L-1} H_{x,x+1}. \quad (5)$$

Here periodic boundary conditions were assumed, i.e. $H_{2L-1,2L} = H_{2L-1,0}$. A simple example of such a model is the Heisenberg spin-chain model [9] with the Hamiltonian

$$H_{\text{HB}}(\vec{J}) = - \sum_{x=0}^{2L-1} (J_1 S_x^1 S_{x+1}^1 + J_2 S_x^2 S_{x+1}^2 + J_3 S_x^3 S_{x+1}^3). \quad (6)$$

The S_i are the three spin operators for spin- $\frac{d-1}{2}$ systems. The sum in a Hamiltonian of the form (5) can be rearranged to

$$H = \sum_{x=0}^{L-1} H_{2x,2x+1} + \sum_{x=0}^{L-1} H_{2x+1,2x+2} = H_e + H_o, \quad (7)$$

where the indices e and o are short for even and odd respectively. We split our Hamiltonian into a sum of two. Note that the terms in each individual sum commute. We can insert (7) into (3) and by choosing t small enough we obtain

$$\mathbb{U}(t) = e^{-iHt} \approx e^{-iH_o t} e^{-iH_e t} = \mathbb{U}_o \mathbb{U}_e, \quad (8)$$

where we define the time-evolutions to be

$$\mathbb{U}_e := \bigotimes_{x=0}^{L-1} e^{-itH_{2x,2x+1}} \quad (9)$$

$$\mathbb{U}_o := \bigotimes_{x=0}^{L-1} e^{-itH_{2x+1,2x+2}}. \quad (10)$$

We can apply multiple time-steps (8) to cover any finite time interval T . This gives us

$$\mathbb{U}(T) \approx (\mathbb{U}_o \mathbb{U}_e)^{\frac{T}{t}} = \left(\bigotimes_{x=0}^{L-1} e^{-itH_{2x+1,2x+2}} \cdot \bigotimes_{x=0}^{L-1} e^{-itH_{2x,2x+1}} \right)^{\frac{T}{t}}. \quad (11)$$

Our overall time-evolution $\mathbb{U}(T)$ to the final time T is split into $\frac{T}{t}$ steps. For each step we have two substeps. In the first we apply a unitary time-evolution to every subsystem with an even index and the system to its right. The second substep applies the evolution to every subsystem with an odd index and the system to its right. This is a little hard to picture, so it is reasonable to develop a good visualisation. We will proceed with that development in the next section.

4 Dual Unitary Operators

4.1 Visualisation and Definition

There is one thing to note before going into the visualisation as proposed in [1]. While we assumed \mathbb{U}^e and \mathbb{U}^o to have the form (9), the discussion later on allows for more general operators

$$\mathbb{U}_e = \bigotimes_{x=0}^{L-1} U_{(2x,2x+1)} \quad (12)$$

$$\mathbb{U}_o = \bigotimes_{x=0}^{L-1} U_{(2x+1,2x+2)}, \quad (13)$$

where $U_{(x,y)} \in \text{End}(\mathcal{H}_x \otimes \mathcal{H}_y)$ are unitary. Each of the two Hilbert spaces has a basis of the form $\{|i\rangle_x \mid i \in I_0(\dim(\mathcal{H}_x) - 1)\}$. Thus we can describe each system using a separate index. This allows us to express $U_{(x,y)}$ as a 4-tensor with the tensor elements defined as

$$(U_{(x,y)})_{ij}^{mn} = \langle m|_x \otimes \langle n|_y U |i\rangle_x \otimes |j\rangle_y. \quad (14)$$

To ease notation the indices x and y indicating which subsystems are acted upon are usually left out unless explicitly required. In common tensor network fashion [10] we may represent U and U^\dagger graphically as

$$\begin{array}{c} m \\ \diagup \quad \diagdown \\ \color{red}{\square} \\ \diagdown \quad \diagup \\ i \quad j \end{array} = U_{ij}^{mn} \qquad \begin{array}{c} m \\ \diagup \quad \diagdown \\ \color{blue}{\square} \\ \diagdown \quad \diagup \\ i \quad j \end{array} = (U^\dagger)_{ij}^{mn} = (U_{mn}^{ij})^* . \quad (15)$$

Note that, while symmetric symbols were used, the operators need not be symmetric in any way and the indices are usually left out of the tensor network diagrams. We redefine \mathbb{U} to be exact in terms of \mathbb{U}_e and \mathbb{U}_o and visualize one time-step (8) as

$$\mathbb{U} = \mathbb{U}^o \mathbb{U}^e = \begin{array}{c} \color{red}{\square} \quad \color{red}{\square} \quad \color{red}{\square} \quad \color{red}{\square} \quad \color{red}{\square} \\ \diagdown \quad \diagup \quad \diagdown \quad \diagup \quad \diagdown \quad \diagup \quad \diagdown \quad \diagup \quad \diagdown \quad \diagup \\ \color{red}{\square} \quad \color{red}{\square} \quad \color{red}{\square} \quad \color{red}{\square} \quad \color{red}{\square} \\ 0 \quad 1 \quad 2 \quad 3 \quad 4 \quad 5 \quad 6 \quad 7 \quad 8 \quad 9 \quad x \end{array} . \quad (16)$$

The dotted line represents the periodic boundary conditions, where the subsystem 0 is equal to the subsystem $2L$, in this case $L = 5$. We can again combine multiple time-steps to reach later times

$$\mathbb{U}^t = \begin{array}{c} t \\ \color{red}{\square} \quad \color{red}{\square} \quad \color{red}{\square} \quad \color{red}{\square} \quad \color{red}{\square} \\ \diagdown \quad \diagup \quad \diagdown \quad \diagup \quad \diagdown \quad \diagup \quad \diagdown \quad \diagup \quad \diagdown \quad \diagup \\ \color{red}{\square} \quad \color{red}{\square} \quad \color{red}{\square} \quad \color{red}{\square} \quad \color{red}{\square} \\ 7/2 \\ \color{red}{\square} \quad \color{red}{\square} \quad \color{red}{\square} \quad \color{red}{\square} \quad \color{red}{\square} \\ \diagdown \quad \diagup \quad \diagdown \quad \diagup \quad \diagdown \quad \diagup \quad \diagdown \quad \diagup \quad \diagdown \quad \diagup \\ \color{red}{\square} \quad \color{red}{\square} \quad \color{red}{\square} \quad \color{red}{\square} \quad \color{red}{\square} \\ 5/2 \\ \color{red}{\square} \quad \color{red}{\square} \quad \color{red}{\square} \quad \color{red}{\square} \quad \color{red}{\square} \\ \diagdown \quad \diagup \quad \diagdown \quad \diagup \quad \diagdown \quad \diagup \quad \diagdown \quad \diagup \quad \diagdown \quad \diagup \\ \color{red}{\square} \quad \color{red}{\square} \quad \color{red}{\square} \quad \color{red}{\square} \quad \color{red}{\square} \\ 3 \\ \color{red}{\square} \quad \color{red}{\square} \quad \color{red}{\square} \quad \color{red}{\square} \quad \color{red}{\square} \\ \diagdown \quad \diagup \quad \diagdown \quad \diagup \quad \diagdown \quad \diagup \quad \diagdown \quad \diagup \quad \diagdown \quad \diagup \\ \color{red}{\square} \quad \color{red}{\square} \quad \color{red}{\square} \quad \color{red}{\square} \quad \color{red}{\square} \\ 3/2 \\ \color{red}{\square} \quad \color{red}{\square} \quad \color{red}{\square} \quad \color{red}{\square} \quad \color{red}{\square} \\ \diagdown \quad \diagup \quad \diagdown \quad \diagup \quad \diagdown \quad \diagup \quad \diagdown \quad \diagup \quad \diagdown \quad \diagup \\ \color{red}{\square} \quad \color{red}{\square} \quad \color{red}{\square} \quad \color{red}{\square} \quad \color{red}{\square} \\ 1 \\ \color{red}{\square} \quad \color{red}{\square} \quad \color{red}{\square} \quad \color{red}{\square} \quad \color{red}{\square} \\ \diagdown \quad \diagup \quad \diagdown \quad \diagup \quad \diagdown \quad \diagup \quad \diagdown \quad \diagup \quad \diagdown \quad \diagup \\ \color{red}{\square} \quad \color{red}{\square} \quad \color{red}{\square} \quad \color{red}{\square} \quad \color{red}{\square} \\ 1/2 \\ \color{red}{\square} \quad \color{red}{\square} \quad \color{red}{\square} \quad \color{red}{\square} \quad \color{red}{\square} \\ 0 \\ 0 \quad 1 \quad 2 \quad 3 \quad 4 \quad 5 \quad 6 \quad 7 \quad 8 \quad 9 \quad 10 \quad x \end{array} , \quad (17)$$

where t is now the number of time steps. We thus have achieved a nice visual representation of the time-evolution of a 1D-chain of length $L2$ of quantum mechanical systems \mathcal{H}_x . For simplicity we assume \mathcal{H}_x to be the same at every site x . We will later on use space-time coordinates (x, t) which are quite self-explanatory with respect to the above visualisation. Whenever we use space- and time-coordinates to describe a position in

such space-time lattices, we will call them events. When only the spatial component x is used, we will stick to calling them sites.

After this is out of the way, we can finally get to the definition of dual unitary operators. Summing up the definitions in [1]:

Def. 1. Let \mathcal{H}_{loc} be a Hilbert space of finite dimension d with basis $\{|j\rangle \mid j \in I_0(d-1)\}$. The **dual operator** \tilde{U} of an operator $U \in \text{End}(\mathcal{H}_{loc}^{\otimes 2})$ is defined via

$$\langle m| \otimes \langle n|\tilde{U}|i\rangle \otimes |j\rangle := \langle j| \otimes \langle n|U|i\rangle \otimes |m\rangle. \quad (18)$$

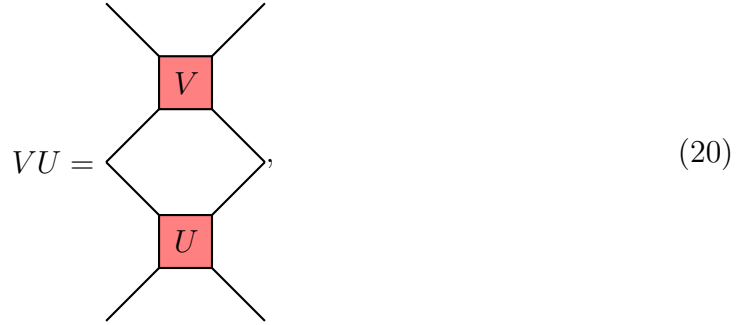
An operator U is called **dual unitary** if both U and \tilde{U} are unitary.

For $d = 2$ we can use an explicit matrix representation and get

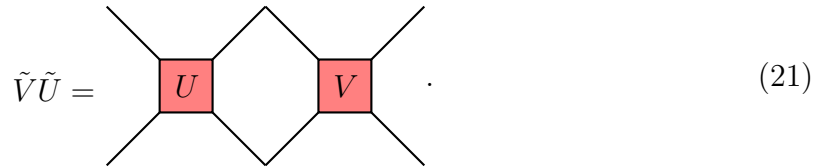
$$U = \begin{pmatrix} u_{00} & u_{01} & u_{02} & u_{03} \\ u_{10} & u_{11} & u_{12} & u_{13} \\ u_{20} & u_{21} & u_{22} & u_{23} \\ u_{30} & u_{31} & u_{32} & u_{33} \end{pmatrix}$$

$$\tilde{U} = \begin{pmatrix} u_{00} & \color{red}u_{20} & u_{02} & \color{blue}u_{22} \\ u_{10} & \color{green}u_{30} & u_{12} & \color{blue}u_{32} \\ \color{red}u_{01} & u_{21} & \color{blue}u_{03} & u_{23} \\ \color{green}u_{11} & u_{31} & \color{blue}u_{13} & u_{33} \end{pmatrix}. \quad (19)$$

The colours show which elements changed position with each other. Intuitively the duality exchanges the role of time and space: While the product of two operators U and V is the following contraction



the product of their duals corresponds to



Note that the tildes in the tensor network diagram were not forgotten, since in the diagram the correct multiplication of dual tensors can be achieved by using the original

tensors and contracting a different combinations of legs compared to the usual multiplication. Assuming time and space are along the same axes as before, we may visualise the two conditions used for a dual unitary operator U . The usual unitary condition

$$UU^\dagger = U^\dagger U = \mathbb{1} \hat{=} \begin{array}{c} \text{---} \\ \diagup \quad \diagdown \\ \square_{\text{blue}} \\ \diagdown \quad \diagup \\ \text{---} \\ \square_{\text{red}} \\ \diagup \quad \diagdown \\ \text{---} \end{array} = \begin{array}{c} \text{---} \\ \diagup \quad \diagdown \\ \square_{\text{red}} \\ \diagdown \quad \diagup \\ \text{---} \\ \square_{\text{blue}} \\ \diagup \quad \diagdown \\ \text{---} \end{array} = \begin{array}{c} \text{---} \\ \diagup \quad \diagdown \\ \text{---} \\ \diagdown \quad \diagup \\ \text{---} \end{array} \quad (22)$$

and the dual unitary condition

$$\begin{array}{c} \tilde{U}\tilde{U}^\dagger = \mathbb{1} \hat{=} \begin{array}{c} \text{---} \\ \diagup \quad \diagdown \\ \square_{\text{blue}} \\ \diagdown \quad \diagup \\ \text{---} \\ \square_{\text{red}} \\ \diagup \quad \diagdown \\ \text{---} \end{array} = \begin{array}{c} \text{---} \\ \diagup \quad \diagdown \\ \text{---} \\ \diagdown \quad \diagup \\ \text{---} \end{array} \\ \tilde{U}^\dagger\tilde{U} = \mathbb{1} \hat{=} \begin{array}{c} \text{---} \\ \diagup \quad \diagdown \\ \square_{\text{blue}} \\ \diagdown \quad \diagup \\ \text{---} \\ \square_{\text{red}} \\ \diagup \quad \diagdown \\ \text{---} \end{array} = \begin{array}{c} \text{---} \\ \diagup \quad \diagdown \\ \text{---} \\ \diagdown \quad \diagup \\ \text{---} \end{array} \end{array} \quad (23)$$

Details on the folding of the product of the dual operators and explicit calculations with indices can be found in the supplementary material of [1]. Before using these newly found concepts to compute interesting properties, there is one more thing to think about. Do dual unitary operators actually exist? The answer is yes and here are two examples:

Example 1. For the qubit-case, i.e. $d = 2$, the **SWAP**-gate on two qubits is a dual unitary operator. It is actually self-dual

$$\mathbf{SWAP} = \begin{pmatrix} 1 & 0 & 0 & 0 \\ 0 & 0 & 1 & 0 \\ 0 & 1 & 0 & 0 \\ 0 & 0 & 0 & 1 \end{pmatrix} = \widetilde{\mathbf{SWAP}}. \quad (24)$$

This fact that can easily be seen from its visualisation

$$\mathbf{SWAP} = \begin{array}{c} \text{---} \\ \diagup \quad \diagdown \\ \text{---} \\ \diagdown \quad \diagup \\ \text{---} \end{array} \quad (25)$$

Therefore $\mathbf{SWAP}^2 = \mathbb{1}$ implies the dual unitarity.

Example 2. We can find a class of dual unitaries using the nearest neighbour interactions of the XXZ-model for $d = 2$. The model is described by the nearest neighbour Hamiltonian [11]

$$H_{XXZ}^{(j,j+1)}[J', J] = J' (\sigma_j^x \otimes \sigma_{j+1}^x + \sigma_j^y \otimes \sigma_{j+1}^y) + J \sigma_j^z \otimes \sigma_{j+1}^z, \quad (26)$$

which is a special case of the aforementioned Heisenberg model (6). We can describe the nearest neighbour interaction by [11]

$$U_{XXZ}[J', J] = e^{-iH_{XXZ}^{(j,j+1)}[J', J]}. \quad (27)$$

$U_{XXZ}[J', J]$ is dual unitary for $J' = \frac{\pi}{4}$. We will see why in a second.

A parametrisation of all dual unitary gates with $d = 2$ can be used to show the dual unitarity of our second example. Such a parametrisation was found in [1]:

Property 1. There exists a parametrisation for all dual unitary operators for the qubit case $d = 2$. It is given by

$$U = e^{i\phi}(u_+ \otimes u_-)V[J](v_- \otimes v_+), \quad (28)$$

with $\phi, J \in \mathbb{R}$, $u_{\pm}, v_{\pm} \in SU(2)$ and

$$V[J] = \exp \left[-i \left(\frac{\pi}{4} \sigma^x \otimes \sigma^x + \frac{\pi}{4} \sigma^y \otimes \sigma^y + J \sigma^z \otimes \sigma^z \right) \right]. \quad (29)$$

The proof is detailed in the supplemental material of [1]. We can find the parameters for our two examples.

1. For the **SWAP**-gate $v_{\pm}, u_{\pm} = \mathbb{1}$ and $\phi, J = \frac{\pi}{4}$. Thus

$$\mathbf{SWAP} = e^{i\frac{\pi}{4}} V \left[\frac{\pi}{4} \right]. \quad (30)$$

2. By comparing (28) and (27) we can clearly see that [1]

$$U_{XXZ} \left[\frac{\pi}{4}, J \right] = V[J] \quad (31)$$

and thus it is a dual unitary operator with $v_{\pm}, u_{\pm} = \mathbb{1}$ and $\phi = 0$.

Let the set of dual unitaries of local dimension d be denoted by $\mathcal{DU}(d)$ and shorten $\mathcal{DU} := \mathcal{DU}(2)$.

4.2 Correlation Functions in 1+1 Dimensions

We will now proceed to a computation that gives a first glimpse at the usefulness of dual unitary operators. The quantity to be computed is the dynamical correlation function of local operators in the infinite temperature state. It is defined as

$$D^{\alpha\beta}(x, y, t) = \frac{1}{d^{2L}} \text{Tr}[a_x^\alpha \mathbb{U}^{-t} a_y^\beta \mathbb{U}^t], \quad (32)$$

with $x, y \in I_0(2L - 1)$, $t \in \mathbb{N}$, and $\{a_x^\alpha\}$ being a basis of the space of local operators at site x . This computation has already been done in [1] and our calculations will be very similar. However, in the process we will stray away from the visual proof as it is done in [1] and give more abstract arguments in parallel. This is to aid in the later sections, where a proper visualisation is harder to achieve and more abstract methods are necessary. We can visualise (32) as

$$D^{\alpha\beta}(x, y, t) = \frac{1}{d^{2L}}$$

$$(33)$$

The first trick is to choose the a^α as Hilbert-Schmidt orthonormal $\text{Tr}[a^\alpha a^\beta] = d\delta_{\alpha\beta}$ and $a^0 = \mathbb{1}$. This implies

$$\text{Tr}[a_x^\alpha] = d\delta_{\alpha,0}. \quad (34)$$

The existence of such a basis follows from the fact that all linear operators on a finite dimensional Hilbert space are Hilbert-Schmidt operators. More information on those can be found in [12].

First we look at the easy case with $\alpha = 0$. This implies

$$D^{0\beta}(x, y, t) = \frac{1}{d^{2L}} \text{Tr}[\mathbb{U}^{-t} a_y^\beta \mathbb{U}^t] = \frac{1}{d} \text{Tr}[a_y^\beta] = \delta_{0,\beta}, \quad (35)$$

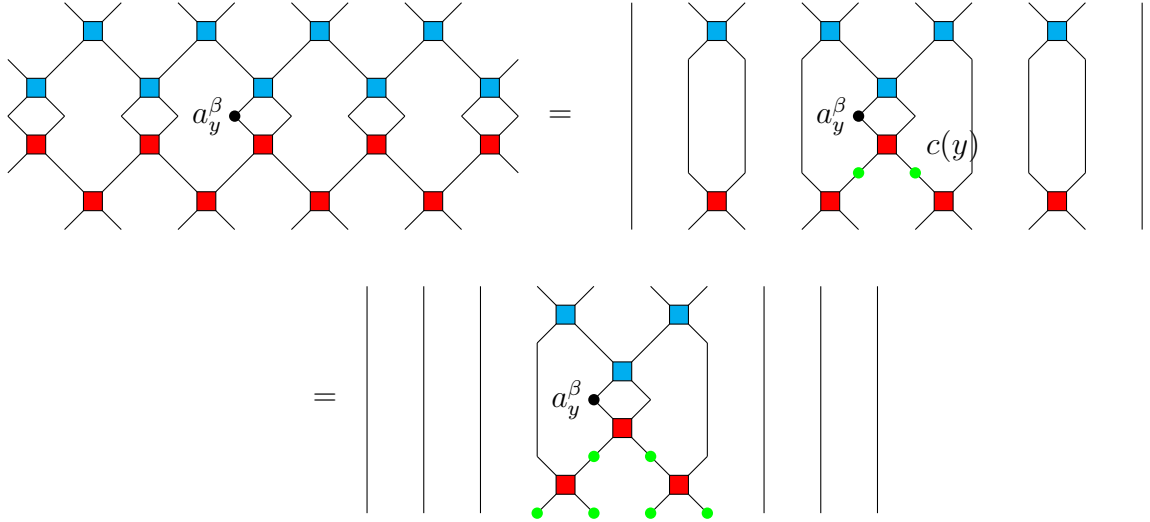


Figure 1: Visualisation of the method to find \mathcal{LC} . The blocked events, i.e. those that are in \mathcal{LC} are marked in green. In each step the usual unitary condition (22) is used.

where the cyclicity of the trace was used for the second equality. Analogously if $\beta = 0$, we find $D^{\alpha 0}(x, y, t) = \delta_{\alpha 0}$.

We will now assume $\alpha, \beta \neq 0$. One could follow [1] and just use the usual unitary condition (22) wherever possible to immediately get a light-cone structure. But we will do this step by step. To do so we want to find the set \mathcal{LC} of events that are such that operators applied on them cannot be contracted with their hermitian conjugate to the identity via the usual unitary condition (22). Furthermore let $\mathcal{LC}(\tau)$ be the set of sites such that for $z \in \mathcal{LC}(\tau)$, $(z, \tau) \in \mathcal{LC}$. While reading the next few lines, it is helpful to refer to Fig. 1, where the first three steps of the method are visualised. We begin at time $\tau = t$, where we apply a_y^β at site y . Thus for all $U_{(2k+1, 2k+2)}$ with $y \in \{2k+1, 2k+2\}$ applied at time $\tau = t - \frac{1}{2}$ we cannot make use of (22). There is exactly one such k and it is such that

$$\{2k+1, 2k+2\} = \left\{ 2 \left\lceil \frac{y}{2} \right\rceil - 1, 2 \left\lceil \frac{y}{2} \right\rceil \right\} =: c(y). \quad (36)$$

Thus $\mathcal{LC}(t - \frac{1}{2}) = c(y)$. Now we continue this to the next time-step, where we cannot apply the usual unitary condition (22) for $U_{(2k, 2k+1)}$ applied at time $\tau = t - 1$, if $\{2k, 2k+1\} \cap c(y) \neq \emptyset$. For the next time-step the condition would be $\{2k+1, 2k+2\} \cap (\{\min c(y) - 1, \max c(y) + 1\} \cup c(y)) \neq \emptyset$. This will continue until we reach $\tau = 0$. Due to our odd-even-change in the application of the dual unitaries the set $\mathcal{LC}(\tau)$ of what we may call blocked sites increases by one to the right and left each for every step we move backwards in time. This gives us the recursion relation

$$\mathcal{LC} \left(\tau - \frac{1}{2} \right) = \mathcal{LC}(\tau) \cup \left\{ z \in I_0(2L-1) \mid \max_{\tilde{y} \in \mathcal{LC}(\tau)} |z - \tilde{y}| = 1 \right\}, \quad (37)$$

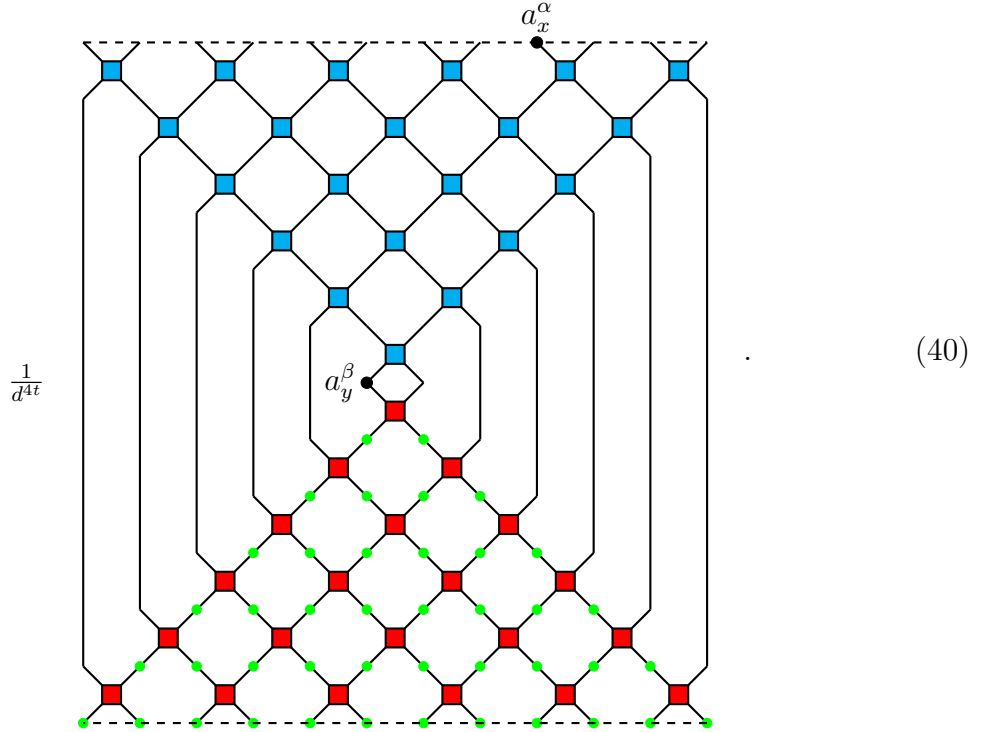
with $\mathcal{LC}(\tau - \frac{1}{2}) = c(y)$ as base case. We can solve the recursion and get

$$\mathcal{LC}(\tau) = \left\{ z \in I_0(2L - 1) \mid \max_{\tilde{y} \in c(y)} |z - \tilde{y}| \leq (2t - 1) - 2\tau \right\}. \quad (38)$$

Thus we find

$$\begin{aligned} \mathcal{LC} &= \bigcup_{\tau \in I_0(t-1)/2} \mathcal{LC}(\tau) \\ &= \left\{ (z, \tau) \in I_0(2L - 1) \times I_0(2t - 1)/2 \mid \min_{\tilde{y} \in c(y)} |z - \tilde{y}| \leq (2t - 1) - 2\tau \right\}, \end{aligned} \quad (39)$$

which has a light-cone-like structure. If we apply (22) to all operators that do not act on an event in \mathcal{LC} , our visual representation (33) changes to



The events in \mathcal{LC} are marked in green. Note that we immediately get the result

$$D^{\alpha\beta}(x, y, t) \propto \text{Tr}[a_x^\alpha] = 0 \quad \text{for} \quad \min_{\tilde{y} \in c(y)} |x - \tilde{y}| > 2t - 1. \quad (41)$$

Up to now we did not need the dual unitary property and the analysis done is true for all unitary operators.

From here on we assume that $L \geq 2t$. If we further assume $|x - y| \leq 2t - 1$, there exists

a structure of the form

(42)

or possibly its mirror image, for $z \in \mathcal{LC}(0)$ such that $|z - y| = 2t - 1$. So it occurs at one of the sides of the light-cone. By assumption the single-site operator a_x^α is not applied at the event $(z, 0)$. Therefore we can apply the dual unitary condition (23). As we can see in (42), this results in a similar structure, but at a later time and a site closer to y . By applying the dual unitary condition $2t - 2$ more times, we get

(43)

or its mirror image. We can thus apply the dual unitary condition (23) one last time, which implies

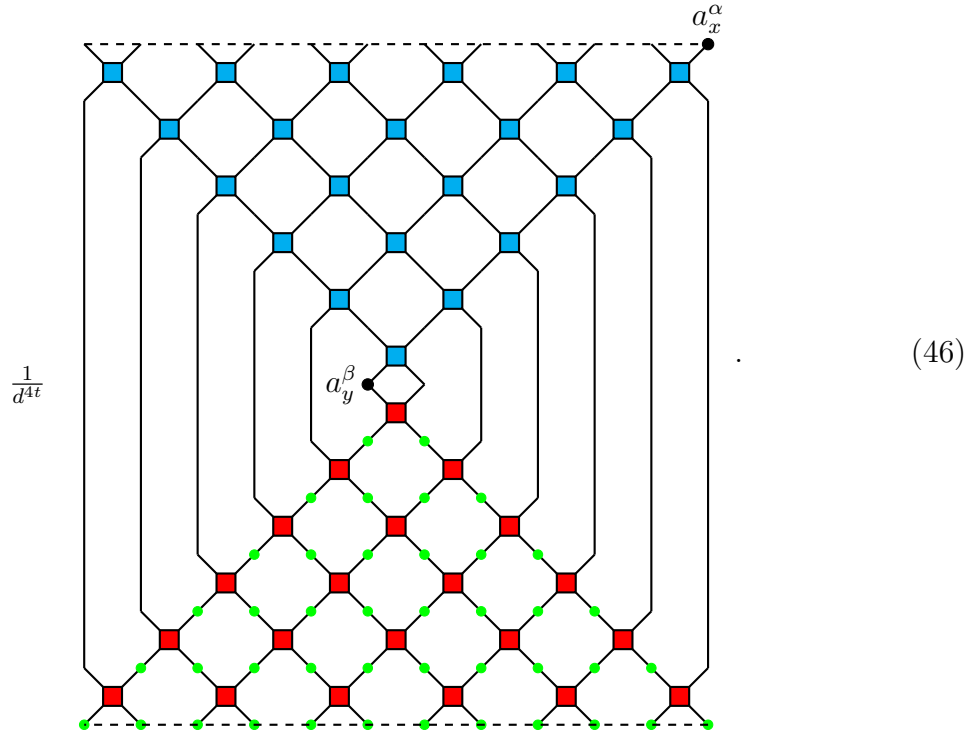
$$D^{\alpha\beta}(x, y, t) \propto \text{Tr} [a_y^\beta] = 0. \tag{44}$$

This leaves us with one remaining position x to examine: $|x - y| = 2t$ and $x \in \mathcal{LC}(0)$. As said earlier, in this case we can't use the iterative application of the dual unitary condition (23) to get (44) in the end. If we start from the same side as before, the operator a_x^α will block the first use of the dual unitary condition. If we start from the other side, we end up with

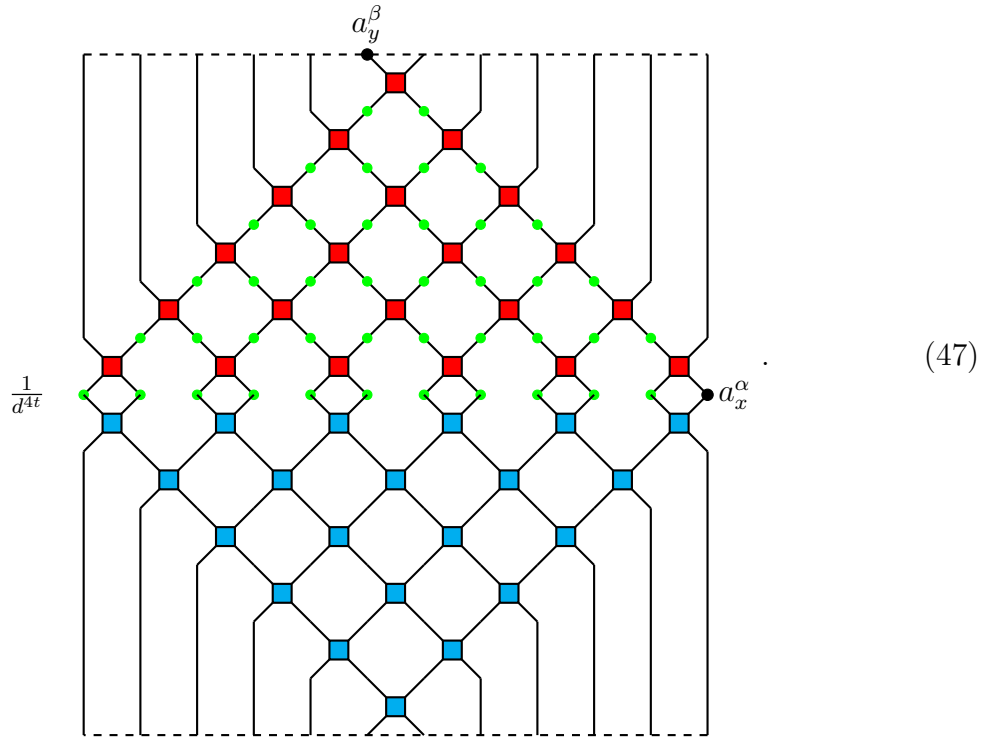
(45)

after $(2t - 1)$ -many applications of the dual unitary condition (23). Thus a_y^β will block the last application of the condition. The visualisation with the last remaining possibility

of x looks like



While we could use the dual unitary condition (23) to proceed, we will make use of the normal unitary condition (22) once more and find the light cone of a_x^α . The visualization can be shifted for convenience, which is basically making use of the cyclicity of the trace in (32). Thus the visualization looks like



Using the same method as for a_y^β earlier, we can get the light-cone of a_x^α as

$$\mathcal{LC}(a_x^\alpha) = \left\{ (z, \tau) \in I_0(2L-1) \times I_1(2t)/2 \mid \min_{\tilde{x} \in c(x)} |z - \tilde{x}| \leq 2\tau - 1 \right\}. \quad (48)$$

Any operator that is not applied to at least one event $(z, \tau) \in (\mathcal{LC}(a_x^\alpha) \cup \{(x, 0)\})$ will become the identity with its hermitian conjugate via (22). So let us determine

$$\mathcal{LC}(a_y^\beta)(\tau) \cap \mathcal{LC}(a_x^\alpha)(\tau). \quad (49)$$

We need to find the sites z such that

$$\min_{\tilde{x} \in c(x)} |z - \tilde{x}| \leq 2\tau - 1 \quad \text{and} \quad \min_{\tilde{y} \in c(y)} |z - \tilde{y}| \leq 2t - 1 - 2\tau. \quad (50)$$

For this task let us assume, that $x < y$. In the case it is not, we reassign the numbering of our sites. This will be required if and only if y is odd, so we may generalise the reassignment as

$$\begin{aligned} R : I_0(2L-1) &\rightarrow R(I_0(2L-1)) \\ z &\mapsto (-1)^y z. \end{aligned} \quad (51)$$

Now let \hat{x} and \hat{y} be such that

$$\hat{y} - \hat{x} = \min_{\substack{\tilde{x} \in c(x) \\ \tilde{y} \in c(y)}} \tilde{y} - \tilde{x} = 2t - 2. \quad (52)$$

These can be found to be given by

$$\begin{aligned} \hat{x} &= x + 1 \\ \hat{y} &= y - 1. \end{aligned} \quad (53)$$

In the case $\hat{x} \leq z \leq \hat{y}$, \hat{x} and \hat{y} will be the sites in $c(x)$ and $c(y)$ respectively with least distance to z . Thus we can determine z via a system of inequalities that are implied by (50) and our assumption on the distance of x and y

$$\begin{aligned} z &\leq \hat{x} + 2\tau - 1 \\ z &\geq \hat{y} - 2t + 1 + 2\tau. \end{aligned} \quad (54)$$

Together with (52) and (53) this results in

$$z = x + 2\tau. \quad (55)$$

Due to periodicity in space, the only other case is $y \leq z \leq x + 2L$ and x and y will be the sites closest to z in $c(x)$ and $c(y)$ respectively. Combining the assumptions $y - x = 2t$ and $2t \leq L$ as well as the restrictions in (50), we find the inequalities

$$z \leq y + 2t - 1 - 2\tau = x + 4t - 1 - 2\tau \leq x + 2L - 1 - 2\tau \quad (56)$$

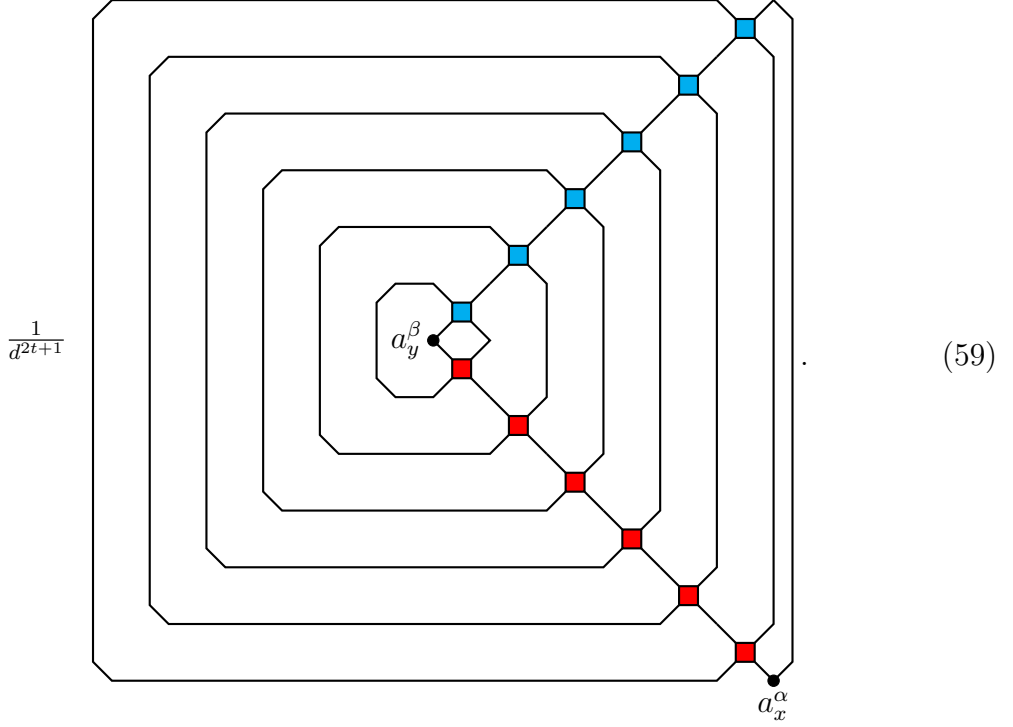
$$z \geq x + 2L - 2\tau + 1. \quad (57)$$

These are clearly contradictory.

Since the above is true for all $\tau \in I_1(2t - 1)/2$, we find that

$$\mathcal{LC}(a_y^\beta) \cap \mathcal{LC}(a_x^\alpha) = \left\{ (z, \tau) \in R(I_0(2L - 1)) \times I_1(2t - 1)/2 \mid z = x + 2\tau \right\}. \quad (58)$$

All operators which are not applied to an event in $(\mathcal{LC}(a_y^\beta) \cap \mathcal{LC}(a_x^\alpha)) \cup \{(x, 0)\}$ will reduce to the identity after applying (22). As R merely changed the assignment, the visualisation now looks like



Now we can define in analogy to [1]

$$M(a, y) = \frac{1}{d} \text{Tr}_2 [\mathbf{SWAP}^y U^\dagger \mathbf{SWAP}^y (\mathbb{1} \otimes a) \mathbf{SWAP}^y U \mathbf{SWAP}^y], \quad (60)$$

to shorten our final result. The SWAP-gates are used to handle the difference between odd and even sides. Visually we find

$$M(a, 2l) = \frac{1}{d} \begin{array}{c} \text{Diagram: A central octagon with a black dot labeled 'a' inside. It is surrounded by a blue square on top and a red square on the bottom, both connected to the octagon's vertices. The entire structure is enclosed in a larger octagonal frame. } \end{array} \quad (61)$$

and

$$M(a, 2l + 1) = \frac{1}{d} \left[\text{Diagram 1} \right] = \frac{1}{d} \left[\text{Diagram 2} \right]. \quad (62)$$

Here the difference between an even and an odd y is easy to spot. Using M we may write

$$D^{\alpha\beta}(x, y, t) = \frac{1}{d} \text{Tr} [M^{2t} (a_y^\beta, y) a_x^\alpha]. \quad (63)$$

While in [1] they explicitly differentiated two different cases, we hid this in the assignment R and the mod2 of y . This may obscure the light-cone and speed analogy made in [1], but will prove helpful in higher dimensions. Let's summarize the results for the correlation function gained in this section

$$D^{\alpha\beta}(x, y, t) = \begin{cases} \delta_{0\beta} & \text{if } \alpha = 0 \\ \delta_{\alpha 0} & \text{if } \beta = 0 \\ 0 & \text{if } x \neq y + (-1)^{y+1}2t \text{ and } \alpha, \beta \neq 0 \\ \frac{1}{d} \text{Tr} [M^{2t} (a_y^\beta, y) a_x^\alpha] & \text{if } x = y + (-1)^{y+1}2t \text{ and } \alpha, \beta \neq 0 \end{cases}. \quad (64)$$

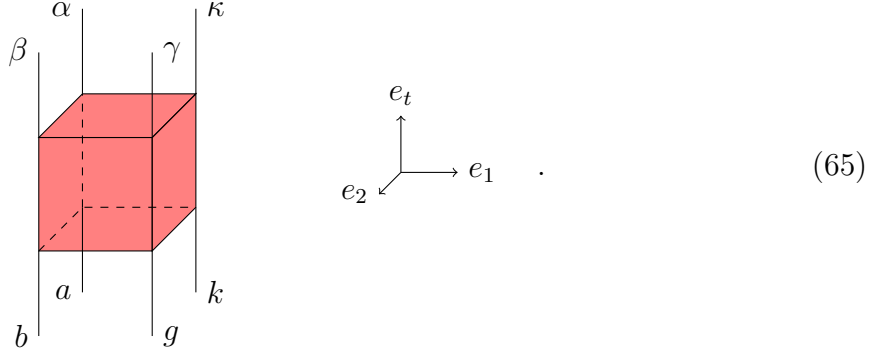
5 Ternary Unitary Operators

5.1 The Set of Ternary Unitaries

At the end of [1] some ideas on generalisations of dual unitary gates and the exact correlation functions were suggested. One of these was the generalisation to multiple dimensions. A more precise construction and computation for $(2 + 1)$ -space-time was made in [13]. However, the gates they used are unitary only in one of the two spacial directions, so one can still call them dual unitary. The construction allows for exact results and leads to light-cone-like structures of correlation functions.

We will now take a different approach and look at operators that are unitary along both space directions. Such operators will need to act on four local systems and we may dub them *ternary unitary operators*. In general we can visualise operators acting on a system

of the form $\mathcal{H}_{\text{loc}}^{\otimes 4}$ as a cube



This leads us to view the operator U as an 8-tensor. As the name suggests 8-tensors are described using 8 indices. If $\{|i\rangle | i \in I_0(d-1)\}$ is a basis of \mathcal{H}_{loc} , we find the tensor elements to be

$$U_{abgk}^{\alpha\beta\gamma\kappa} = \langle \alpha\beta\gamma\kappa | U | abgk \rangle. \quad (65)$$

Now we can properly define ternary unitary operators.

Def. 2. Let \mathcal{H}_{loc} be a Hilbert space of finite dimension d . An operator $U \in \text{End}(\mathcal{H}_{\text{loc}}^{\otimes 4})$ is called a **ternary unitary** if and only if

$$\sum_{\alpha\beta\gamma\kappa} U_{abgk}^{\alpha\beta\gamma\kappa} (U^*)_{\tilde{a}\tilde{b}\tilde{g}\tilde{k}}^{\alpha\beta\gamma\kappa} = \delta_{abgk, \tilde{a}\tilde{b}\tilde{g}\tilde{k}} \quad (67)$$

$$\sum_{ab\alpha\beta} U_{abgk}^{\alpha\beta\gamma\kappa} (U^*)_{ab\tilde{g}\tilde{k}}^{\alpha\beta\tilde{\gamma}\tilde{\kappa}} = \delta_{gk, \tilde{g}\tilde{k}} \quad (68)$$

$$\sum_{ak\alpha\kappa} U_{abgk}^{\alpha\beta\gamma\kappa} (U^*)_{\tilde{a}\tilde{b}\tilde{g}\tilde{k}}^{\alpha\tilde{\beta}\tilde{\gamma}\kappa} = \delta_{bg, \tilde{b}\tilde{g}}. \quad (69)$$

We denote the set of ternary unitary operators for local dimension d as $\mathcal{TU}(d)$.

Each of the three conditions merely describes a unitary condition along one of the three coordinate axes. The three conditions imply each a unitary condition in direction opposite to the coordinate axes. Instead of explicitly using tensor elements, we can define two new operators as follows:

$$\langle gk\gamma\kappa | \tilde{U} | ab\alpha\beta \rangle = \langle \alpha\beta\gamma\kappa | U | abgk \rangle \quad (70)$$

$$\langle bg\beta\gamma | \bar{U} | ak\alpha\kappa \rangle = \langle \alpha\beta\gamma\kappa | U | abgk \rangle. \quad (71)$$

To define an operator U to be a ternary unitary if and only if U , \tilde{U} and \bar{U} are unitary, is equivalent to the above definition 2. Note that equation (67) is just the normal unitary condition along the time direction $UU^\dagger = \mathbb{1}$, which implies $U^\dagger U = \mathbb{1}$. We may visualise

the two as

(72)

where U is the red and U^\dagger the blue cube. Equation (68) is the unitary condition along the e_1 -direction. It is equivalent to the condition $\tilde{U}\tilde{U}^\dagger = \mathbb{1}$. The later implies the condition $\tilde{U}^\dagger\tilde{U} = \mathbb{1}$. The two can be visualised as

(73)

Finally equation (69) does the same thing for the e_2 -direction and for the operator \bar{U} . The two conditions $\bar{U}\bar{U}^\dagger = \mathbb{1}$ and $\bar{U}^\dagger\bar{U} = \mathbb{1}$ can be visualised as

(74)

Now that these defining properties are established, we may again ask: do any such operators exist? Once more the answer is yes:

Example 3. *If we look at the case of qubits, i.e. $d = 2$, and associate a number to each site in a clockwise fashion, we may consider the permutation*

$$\pi = \begin{pmatrix} 1 & 2 & 3 & 4 \\ 3 & 4 & 1 & 2 \end{pmatrix}. \quad (75)$$

Thus we immediately see that

$$\mathcal{X} \cap \mathcal{Y} \neq \emptyset, \quad (81)$$

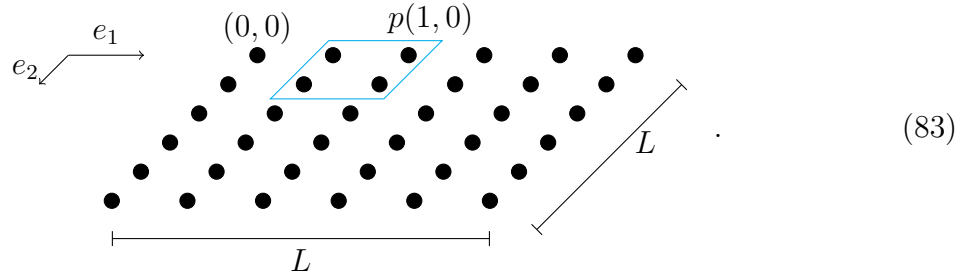
where \mathcal{X} and \mathcal{Y} are the sets of ternary unitary operators gained via the construction X and Y respectively. However, an unsolved question is, if $\mathcal{X} = \mathcal{Y}$ and if all ternary unitaries can be constructed like this.

5.2 Correlation Functions in 2+1 Dimensions

As we now look at (2+1)-space-time dimensions, our overall system is a two-dimensional lattice of sites. To each site its own local Hilbert space \mathcal{H}_{loc} of dimension d is associated. For simplicity we assume both sides of the lattice to consist of $2L$ -many sites, where $L \in \mathbb{N}$. Each site may be described via two coordinates $(i, j) \in I_0(2L-1)^2$. Furthermore U_S denotes that the local operator U is applied to some finite set of sites $S \subset I_0(2L-1)^2$ and the identity is applied to all other sites in $I_0(2L-1)^2$. With regard to our ternary unitaries it is useful to define a plaquette characterised by a site $x = (x_1, x_2)$ as

$$p(x) := \{(x_1, x_2), (x_1 + 1, x_2), (x_1, x_2 + 1), (x_1 + 1, x_2 + 1)\}. \quad (82)$$

The setting may be visualised as



We will once more need to define how we want to time-evolve our system. Thus we first define the two operators

$$U_{ee} = \bigotimes_{(i,j) \in I_0(L-1)^2} U_{p(2i,2j)} \quad (84)$$

$$U_{oo} = \bigotimes_{(i,j) \in I_0(L-1)^2} U_{p(2i+1,2j+1)}, \quad (85)$$

where $U \in \mathcal{TU}(d)$. Graphically from the top-down perspective:

$$U_{ee} = \begin{array}{cccc} \blacksquare & \blacksquare & \blacksquare & \blacksquare \\ \blacksquare & \blacksquare & \blacksquare & \blacksquare \\ \blacksquare & \blacksquare & \blacksquare & \blacksquare \\ \blacksquare & \blacksquare & \blacksquare & \blacksquare \end{array} \quad U_{oo} = \begin{array}{ccccc} \blacksquare & \blacksquare & \blacksquare & \blacksquare & \blacksquare \\ \blacksquare & \blacksquare & \blacksquare & \blacksquare & \blacksquare \\ \blacksquare & \blacksquare & \blacksquare & \blacksquare & \blacksquare \\ \blacksquare & \blacksquare & \blacksquare & \blacksquare & \blacksquare \\ \blacksquare & \blacksquare & \blacksquare & \blacksquare & \blacksquare \end{array}, \quad (86)$$

where the local operators U are marked in red and periodic boundary conditions are assumed. Now we can define one time step of the time-evolution as

$$\mathbb{U} = \mathbb{U}_{oo}\mathbb{U}_{ee}. \quad (87)$$

Why it is chosen like this will be discussed in detail in section 5.3. The correlation function is defined as

$$D^{\alpha\beta}(x, y, t) = \frac{1}{d^{4L^2}} \text{Tr} [a_x^\alpha \mathbb{U}^{-t} a_y^\alpha \mathbb{U}^t], \quad (88)$$

where once more $\{a_x^\alpha\}_{\alpha \in I_0(d^2-1)}$ is a basis of local operators on $\mathcal{H}_x = \mathcal{H}_{\text{loc}}$. Using the same trick as in section 4.2 by choosing $a_x^0 = \mathbb{1}$ and $\text{Tr} [a_x^\alpha a_x^\beta] = d\delta_{\alpha\beta}$, we get

$$\text{Tr} [a_x^\alpha] = d\delta_{\alpha 0}. \quad (89)$$

This immediately gives us the same results as in section 4.2:

$$D^{0\beta}(x, y, t) = \delta_{0\beta}, \quad (90)$$

$$D^{\alpha 0}(x, y, t) = \delta_{\alpha 0} \quad (91)$$

for all x, y and t .

Now assume that $\alpha \neq 0$ and $\beta \neq 0$. We could visualise the correlation function with one single-site operator, then a couple of layers of cubes representing \mathbb{U}^t , again a single-site operator, and finally an equal amount of layers as before representing \mathbb{U}^{-t} . Since this would be rather messy, a different approach will be taken to first simplify the tensor network. To do so we want to determine which operators making up \mathbb{U}^t do not immediately cancel via the usual unitary condition (72) with their hermitian conjugate in \mathbb{U}^{-t} . This is similar to our procedure in section 4.2. It will turn out to be useful to find the set of events these operators are applied to. We will denote this set by \mathcal{LC} . Furthermore, $\mathcal{LC}(\tau)$ will be the set of sites z for which the event (z, τ) is in \mathcal{LC} . To determine \mathcal{LC} we will go layer by layer as visualised in Fig. 2. First we look at the layer at time $\tau = t$. Here, a_y^β is applied as well as \mathbb{U}_{oo}^\dagger . At time $\tau = t - \frac{1}{2}$, \mathbb{U}_{oo} is applied. Now using the unitary-condition in time direction (72), most of the unitaries U in \mathbb{U}_{oo} cancel with their Hermitian conjugate U^\dagger in \mathbb{U}_{oo}^\dagger , except for the one applied on the plaquette $p_m := p(2 \lceil \frac{y_1}{2} \rceil - 1, 2 \lceil \frac{y_2}{2} \rceil - 1)$. In the next earlier time step $\tau = t - 1$, all unitaries of \mathbb{U}_{ee} that are applied to at least one site in p_m will not be trivially connected to their hermitian conjugates in the layer \mathbb{U}_{ee}^\dagger , which is applied at time $t + \frac{1}{2}$. We say they are blocked to cancel with their Hermitian conjugate. These remaining unitaries at time $\tau = t - 1$ in turn block even more sites at earlier times. Due to the odd-even application of the unitaries, the set of blocked sites will increase in each direction by one row with each step to earlier times. $\mathcal{LC}(\tau)$ is precisely the set of blocked sites at time τ . Thus we obtain the recursion relation

$$\mathcal{LC}(\tau) = \mathcal{LC}\left(\tau + \frac{1}{2}\right) \cup \left\{ z \mid \min_{\tilde{y} \in \mathcal{LC}(\tau + \frac{1}{2})} \|z - \tilde{y}\|_\infty = 1 \right\}, \quad (92)$$

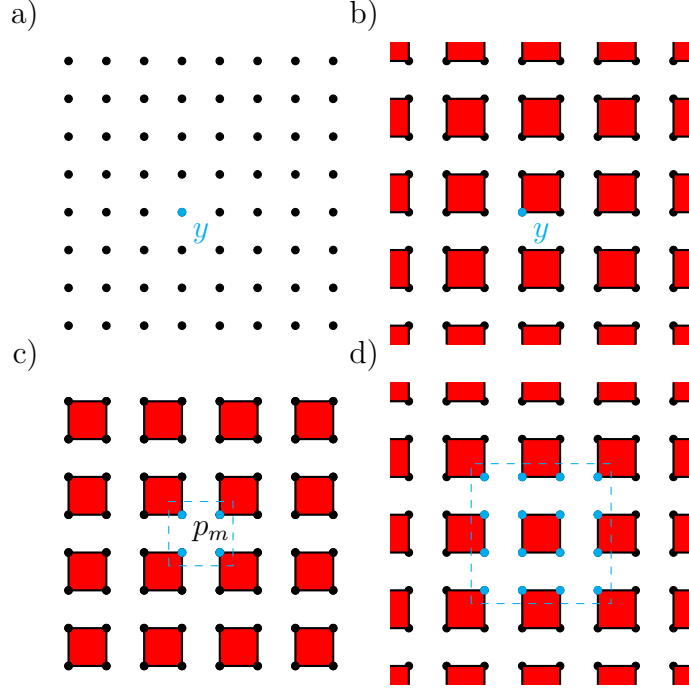


Figure 2: A visualisation of the step by step method. The local operators U are marked in red in each step. a) At time t the operator a_y^β is applied and blocks the site y marked in cyan. b) The operators in a \mathbb{U}_{oo} -layer are applied at time $t - \frac{1}{2}$ and connected to a layer \mathbb{U}_{oo}^{-1} . However, on the blocked site they are not trivially connected. c) After all possible applications of the usual unitary condition (72), the operator applied to p_m at time $t - \frac{1}{2}$ remains, blocking all four sites. Thus operators in the layer \mathbb{U}_{ee} applied at time $t - 1$ and at least partially on sites in p_m are not trivially connected to the corresponding layer in \mathbb{U}_{ee}^{-1} . d) This increases the set of blocked sites for the next earlier time $t - \frac{3}{2}$ further to set $\mathcal{LC}(t - \frac{3}{2})$. Here $\mathcal{LC}(t - \frac{3}{2})$ is marked in cyan.

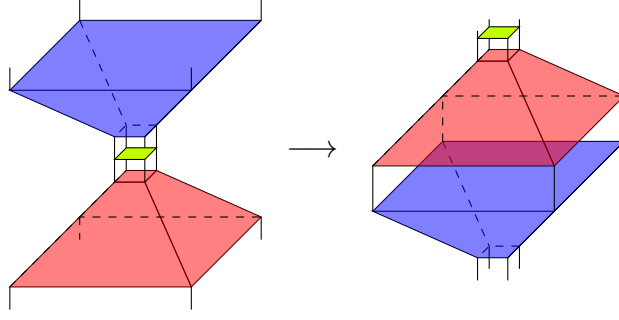


Figure 3: A simplified visualisation of the pyramid-shaped light-cones. As we look at a trace, we can utilise its cyclic property and shift along the time direction. a_y^β could be applied to any of the four sites in the green square, this would be at the time $\tau = t$. a_x^α would be applied somewhere in between the bases of the two pyramids. On the right, we can assign negative times to events that are part of the blue pyramid.

with the initial condition $\mathcal{LC}(t - \frac{1}{2}) = p_m$. Any operator at time τ that is applied to sites in $\mathcal{LC}(\tau)$ will not cancel with its Hermitian conjugate. We can find a solution to the relation as

$$\mathcal{LC}(\tau) = \left\{ z \mid \min_{\tilde{y} \in p_m} \|z - \tilde{y}\|_\infty \leq 2t - 1 - 2\tau \right\}. \quad (93)$$

Thus one arrives at a light-cone given by

$$\mathcal{LC} = \left\{ (z, \tau) \in I_0(2L - 1)^2 \times I_0(2t - 1)/2 \mid \min_{\tilde{y} \in p_m} \|z - \tilde{y}\|_\infty \leq 2t - 1 - 2\tau \right\}. \quad (94)$$

This set has a square pyramid shape with a base length of $4t$ sites. Every unitary $U_{(p,\tau)}$ that is applied to a plaquette $p \subset \mathcal{LC}(\tau)$ of sites at time τ will not cancel with $U_{(p,2t-\tau)}^\dagger$. From this we immediately get the result

$$D^{\alpha\beta}(x, y, t) = 0 \quad \text{if } x \notin \mathcal{LC}(0). \quad (95)$$

So far we have solely used the unitary condition in time and ended up with a light cone structure resembling two pyramids with flat tops. This is visualised on the left in Fig. 3. This would be true even if all the U were only standard unitary operators.

Now assume that $L \geq 2t$ and the remaining operators U are in $\mathcal{TU}(d)$. We may characterize the sides of our light-cone by their distance to two sites in $p_m = \{y^1, y^2, y^3, y^4\}$ as

$$S_{ij}(\tau) = S_{ji}(\tau) = \{z \in \mathcal{LC}(\tau) \mid \|z - y^i\|_\infty = \|z - y^j\|_\infty = 2t - 2\tau\}. \quad (96)$$

In a similar way, we can also characterise the corners of the base z_i via

$$|z_j^i - y_j^i| = 2t \quad \forall j \in \{1, 2\}. \quad (97)$$

Intuitively, z^i is the corner and S_{ij} are the sides furthest away from the site y^i in p_m .

Now assume that $x \neq z^i$ with $y = y^i$. First we make use of the cyclicity of the trace

$$\text{Tr} [a_x^\alpha \mathbb{U}^{-t} a_y^\beta \mathbb{U}^t] = \text{Tr} [a_y^\beta \mathbb{U}^t a_x^\alpha \mathbb{U}^{-t}]. \quad (98)$$

Furthermore we relabel the time-coordinate of events the hermitian conjugates are applied to to be negative, i.e. $\tau \in I_{-1}(-2t)/2$. This is visualised on the right of Fig. 3. The assumption $x \neq z^i$ implies, that we can always find a side $S_{ij}(0)$, such that $x \notin S_{ij}(0)$. We will now examine the ternary unitaries that are applied to at least one site in $S_{ij}(0)$ at time 0 and their corresponding hermitian conjugates applied to the same sites but at time $-\frac{1}{2}$. Due to the matrix multiplication in (98) and as $x \notin S_{ij}(0)$ they are connected via the identity through the sites in $S_{ij}(0)$ at time 0. Due to the trace in (98) the events $(z, \frac{1}{2})$ for $z \in S_{ij}$ are connected to the events $(z, -\frac{1}{2})$ also via the identity. Thus we can apply the appropriate unitary condition in space on them, i.e.

(99)

The sites in $S_{ij}(0)$ are marked by the black dots. This will serve as our base case for the following recursion. For the operators applied at time τ and at least partially on sites in $S_{ij}(0)$, the corresponding hermitian conjugates will be applied at time $-\tau - \frac{1}{2}$. Due to the trace in (98) any event of the form (z, τ) with $z \in S_{ij}(\tau)$ is connected to the

event $(z, -\tau - \frac{1}{2})$ via the identity. If the events (z, τ) and $(z, -\tau)$ are also connected via the identity, we can use one of the spatial unitary conditions (73) or (74), for the aforementioned operators and their hermitian conjugates. This will result in an event of the form $(\tilde{z}, \tau + \frac{1}{2})$, with $\tilde{z} \in S_{ij}(\tau + \frac{1}{2})$, being connected to the event $(\tilde{z}, -\tau - \frac{1}{2})$ via the identity, allowing for the same argument again but for operators applied to the events $(\tilde{z}, \tau + \frac{1}{2})$. This can in short be visualized by

(100)

where the black dots mark the events $(\tilde{z}, \tau + \frac{1}{2})$ and $(\tilde{z}, -\tau - \frac{1}{2})$ for $\tilde{z} \in S_{ij}(\tau + \frac{1}{2})$. In order to reduce cluttering, some of the legs on the operators were left out in both equations. After iterating this condition $2t - 1$ times, including the base case, we have to stop, since $S_{ij}(2t)$ is not defined. Thus we end up with

(101)

The green dots mark the possible positions of the operator a_y^β , i.e. the two sites in p_m that are furthest away from the site we started from. Visually, each time we applied the unitary condition we moved up one step of the pyramid. equation (101) implies that

$$D^{\alpha\beta}(x, y, t) = 0. \quad (102)$$

Finally we look at the case $x = z^i$ for $y = y^i$. So x is the site in $\mathcal{LC}(0)$ furthest away from

y . While we may still find two sides looking like (99) where we can use the appropriate unitary condition, the final step (101) cannot be made, as a_y^β would block the required site, i.e. it would be applied on one of the two sites not marked in green. However, we can solve this problem by simplifying the situation further. In the shifted picture, cf. Fig. 3, it is easy to see that we can once more use the unitary condition in time. In a similar manner as before, we find the light-cone of a_x^α to be

$$\mathcal{LC}(a_x^\alpha) = \left\{ (z, \tau) \in I_0(2L-1)^2 \times I_2(2t)/2 \mid \min_{\tilde{x} \in p_n} \|z - \tilde{x}\|_\infty \leq 2\tau - 1 \right\}, \quad (103)$$

with the plaquette $p_n := p\left(2\lfloor \frac{x_1}{2} \rfloor, 2\lfloor \frac{x_2}{2} \rfloor\right)$. As all the unitary conditions in time can be applied without one resulting in blocking the other, what remains are operators applied to events in

$$\mathcal{C} := (\mathcal{LC}(a_y^\beta) \cap \mathcal{LC}(a_x^\alpha)) \cup \{(x, 0)\}. \quad (104)$$

So we once more have to find the intersection of the two light-cones. For that assume $x_i < y_i$ for all $i \in \{1, 2\}$. If that is not true for some i we may relabel the sites. Since this will be the case if and only if y_i is odd, we can generalize the reassignment as

$$R_i : z_i \mapsto (-1)^{y_i} z_i. \quad (105)$$

All this is very familiar already, as R_i is just R from equation (51) for a certain direction of space. Now let x_n and y_m be such that they are the closest two sites to the other plaquette in p_n and p_m respectively, i.e.

$$\|x_n - y_m\|_\infty = \min_{(\tilde{x}, \tilde{y}) \in p_n \times p_m} \|\tilde{x} - \tilde{y}\| = 2t - 2. \quad (106)$$

We can quickly find that

$$|(x_n)_i - (y_m)_i| = 2t - 2 \quad (107)$$

$$(x_n)_i = x_i + 1 \quad (108)$$

$$(y_m)_i = y_i - 1 \quad (109)$$

and by assumption

$$y_i - x_i = 2t \quad (110)$$

for all i . Now we can see that in each time direction the same constrictions are true independently and that they are exactly the same restrictions as given in section 4.2. Thus by replacing according to

$$\begin{aligned} x_i &\rightarrow x \\ y_i &\rightarrow y \\ z_i &\rightarrow z, \end{aligned} \quad (111)$$

we can reuse our old results, such that

$$z_i = x_i + 2\tau \quad (112)$$

for all i and τ . Therefore

$$\mathcal{C} = \left\{ (z, \tau) \in \bigotimes_{i=1}^2 R_i(I_0(2L-1)) \times I_0(2t-1)/2 \mid z = x + \sum_{i=1}^2 2\tau e_i \right\}. \quad (113)$$

We also know that only operators applied to events in \mathcal{C} do not reduce to the identity with their hermitian conjugate. The result can be visualised as

$$D^{\alpha\beta}(x, y, t) = \frac{1}{d^{6t+1}} \cdot \quad (114)$$

Similar to section 4.2 we can condense this by defining a new operator as follows:

$$M(a, y) = \frac{1}{d^3} \text{Tr}_{(0,1),(1,0),(1,1)} [\mathcal{S}^\dagger(y) U^\dagger \mathcal{S}^\dagger(y) \tilde{a} \mathcal{S}(y) U \mathcal{S}(y)], \quad (115)$$

where $\tilde{a} = \bigotimes_{i,j=0}^1 (\delta_{(i,j),(1,1)} a_{(1,1)} + (1 - \delta_{(i,j),(1,1)}) \mathbb{1}_{(i,j)})$, which means a is always applied at site $(1,1)$ whereas the identity is applied to the remaining sites. Furthermore we define

$$\mathcal{S}(y) = \prod_{i=1}^2 \left(\bigotimes_{j \in \{0,1\}^2, j_i=0} \text{SWAP}_{(\sum_{k=1}^2 j_k e_k, \sum_{k=1}^2 j_k e_k + e_i)} \right)^{y_i}. \quad (116)$$

This time we labelled the grid of four sites as

$$\begin{array}{ccc} (0,0) \bullet & & \bullet (1,0) \\ (0,1) \bullet & & \bullet (1,1) \end{array} \quad e_2 \begin{array}{c} \nearrow \\ \rightarrow \end{array} e_1. \quad (117)$$

Intuitively $\mathcal{S}(y)$ connects the two sites that are neighbours along the e_i direction with a **SWAP**-gate if y_i is odd. This is used to handle the four possible positions the operator

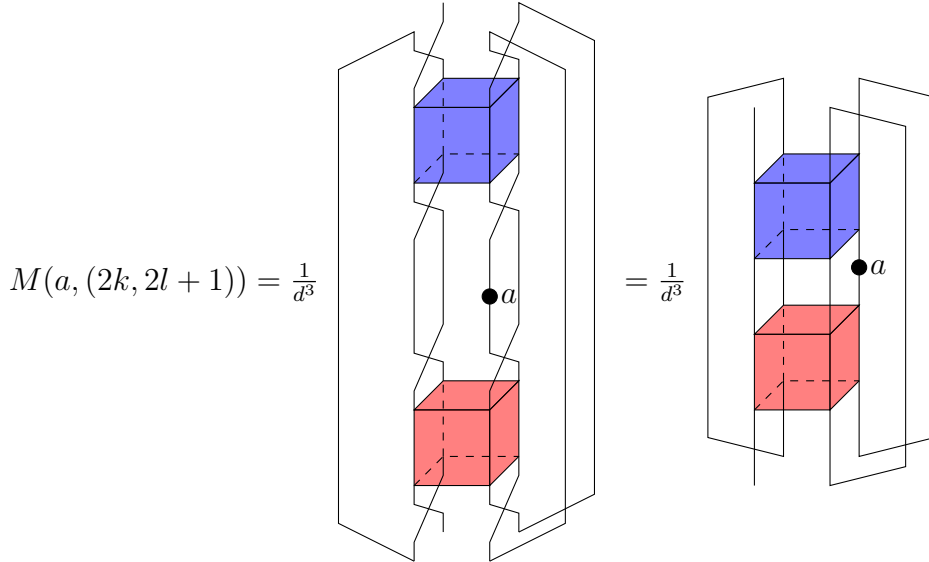


Figure 4: A visualisation of the operator valued linear map $M(a, y)$ for y of the form $(2k, 2l + 1)$ with $k, l \in \mathbb{N}_0$, i.e. it has an even e_1 -coordinate and an odd e_2 -coordinate. We can see how the SWAP-gates act to account for a different site position of a .

a_y^β could be applied to. An example for $y = (2k, 2l + 1)$ is given in figure 4. Note that M is a linear map over $\text{End}(\mathcal{H}_{\text{loc}})$. Using (115), we write the correlation function as

$$D^{\alpha\beta}(x, y, t) = \frac{1}{d} \text{Tr} [M^{2t}(a_y^\beta, y) a_x^\alpha]. \quad (118)$$

We again summarise our results as

$$D^{\alpha\beta}(x, y, t) = \begin{cases} \delta_{0\beta} & \text{if } \alpha = 0 \\ \delta_{\alpha 0} & \text{if } \beta = 0 \\ 0 & \text{if } x \neq y + \sum_{i=1}^2 (-1)^{y_i+1} t e_i \text{ and } \alpha, \beta \neq 0 \\ \frac{1}{d} \text{Tr} [M^t(a_y^\beta, y) a_x^\alpha] & \text{if } x = y + \sum_{i=1}^2 (-1)^{y_i+1} t e_i \text{ and } \alpha, \beta \neq 0 \end{cases}, \quad (119)$$

which are almost the same as for the 1D-case (64).

5.3 Other Time-Evolutions

As mentioned it is not immediately obvious why we chose (87) as our time-evolution. The main reason is that it fits with our motivation via Trotterisation discussed in section 3. However, using this as the only argument, there is a more naive choice for a time-evolution. On the 2D-grid of size $4L^2$, assuming periodic boundary conditions, every site has four neighbours. Thus naively we want to split the Hamiltonian for nearest

neighbour interactions into four parts:

$$\begin{aligned}
H_{\text{nn}} &= \sum_{k \sim l} H_{k,l} \\
&= \sum_{a,b} (H_{(2a,b),(2a+1,b)} + H_{(a,2b),(a,2b+1)} + H_{(2a+1,b),(2a+2,b)} + H_{(a,2b+1),(a,2b+2)}) \\
&= H_{e1} + H_{e2} + H_{o1} + H_{o2},
\end{aligned} \tag{120}$$

where $k \sim l$ denotes the nearest neighbour relation, i.e. that k and l are nearest neighbours. Now we apply the Trotterisation (3) to get

$$e^{-iH_{\text{nn}}t} \approx e^{-iH_{o2}t} e^{-iH_{o1}t} e^{-iH_{e2}t} e^{-iH_{e1}t}, \tag{121}$$

such that we can once more exchange the exponential operators for general unitary operators and define the time-evolution

$$\mathbb{U} = \mathbb{U}_{o2} \mathbb{U}_{o1} \mathbb{U}_{e2} \mathbb{U}_{e1}, \tag{122}$$

where the \mathbb{U}_{ij} are defined using local unitaries similar to (12), (13), (84) and (85). However, we can choose

$$\mathbb{U}_{ee} = \mathbb{U}_{e2} \mathbb{U}_{e1} \tag{123}$$

$$\mathbb{U}_{oo} = \mathbb{U}_{o2} \mathbb{U}_{o1}, \tag{124}$$

as valid operators in the time-evolution (87) of the previous section. This can either be seen via visualisation or by the fact that $\mathbb{U}_{e2} \mathbb{U}_{e1}|_{p(2k,2l)}$ and $\mathbb{U}_{o2} \mathbb{U}_{o1}|_{p(2k+1,2l+1)}$ for $k, l \in I_0(L-1)$ correspond to an operator in $\text{End}(\mathcal{H}^{\otimes 4})$ that has the same structure as the operator in (77) but with general unitary operators and not restricted to those in $\mathcal{DU}(d)$.

Therefore the most naive choice (122) for a time-evolution is already included in our time-evolution (87). As said before we can justify our choice of (87) as a time-evolution via a Trotterisation as well. We need to split the Hamiltonian in a different way

$$\begin{aligned}
H_{\text{nn}} &= \sum_{k \sim l} H_{k,l} \\
&= \sum_{a,b} \left[\left(\sum_{\substack{x,y \in p(2a,2b) \\ x \sim y}} H_{x,y} \right) + \left(\sum_{\substack{x,y \in p(2a+1,2b+1) \\ x \sim y}} H_{x,y} \right) \right] \\
&= H_{ee} + H_{oo},
\end{aligned} \tag{125}$$

which is admittedly more complicated than (121). If we apply the Trotterisation (3) to $H_{\text{nn}} = H_{ee} + H_{oo}$ and repeat the step of replacing exponentials by general unitary operators, we will precisely end up with our usual time-evolution (87) in two spatial dimensions.

Other time-evolutions can be found by defining

$$\mathbb{U}_{eo} = \bigotimes_{(i,j) \in I_0(\frac{l}{2}-1)^2} U_{p(2i,2j+1)} \quad (126)$$

$$\mathbb{U}_{oe} = \bigotimes_{(i,j) \in I_0(\frac{l}{2}-1)^2} U_{p(2i+1,2j)}. \quad (127)$$

These operators act precisely on the plaquettes that are not acted upon by the operators \mathbb{U}_{ee} and \mathbb{U}_{oo} , cf. the definitions (84) and (85). We can visualize the newly defined operators via a top-down perspective

$$\mathbb{U}_{eo} = \begin{array}{cc} \begin{array}{c} | \\ \bullet \\ \hline \bullet \\ | \end{array} & \begin{array}{c} | \\ \bullet \\ \hline \bullet \\ | \end{array} \\ \begin{array}{c} \bullet \\ \hline \bullet \\ \hline \bullet \\ \hline \bullet \\ | \end{array} & \begin{array}{c} \bullet \\ \hline \bullet \\ \hline \bullet \\ \hline \bullet \\ | \end{array} \\ \begin{array}{c} | \\ \bullet \\ \hline \bullet \\ | \end{array} & \begin{array}{c} | \\ \bullet \\ \hline \bullet \\ | \end{array} \end{array} \quad \text{and} \quad \mathbb{U}_{oe} = \begin{array}{cc} \begin{array}{c} \bullet \\ \hline \bullet \\ | \end{array} & \begin{array}{c} \bullet \\ \hline \bullet \\ \hline \bullet \\ \hline \bullet \\ | \end{array} & \begin{array}{c} \bullet \\ \hline \bullet \\ | \end{array} \\ \begin{array}{c} \bullet \\ \hline \bullet \\ \hline \bullet \\ | \end{array} & \begin{array}{c} \bullet \\ \hline \bullet \\ \hline \bullet \\ \hline \bullet \\ | \end{array} & \begin{array}{c} \bullet \\ \hline \bullet \\ | \end{array} \\ \begin{array}{c} \bullet \\ \hline \bullet \\ | \end{array} & \begin{array}{c} \bullet \\ \hline \bullet \\ \hline \bullet \\ | \end{array} & \begin{array}{c} \bullet \\ \hline \bullet \\ | \end{array} \end{array}. \quad (128)$$

From that we can see that

$$\tilde{\mathbb{U}} = \mathbb{U}_{oe} \mathbb{U}_{eo} \quad (129)$$

is equal to (87) for a grid shifted by e_2 . Thus due to periodic boundary conditions the two time-evolutions (87) and (129) are equivalent.

Two more classes of time-evolutions are worth mentioning. An example for the first is

$$\mathbb{U}_{\text{all}} = \mathbb{U}_{oe} \mathbb{U}_{oo} \mathbb{U}_{eo} \mathbb{U}_{ee}. \quad (130)$$

Here we apply in one time-step four gates in a counter-clockwise way around a site with odd-odd coordinates. A visualisation is given in Fig. 5. We can still make the initial step to get a light-cone structure with this time-evolution. But the step where the unitary conditions in space were used, visualized in (99), is not possible. We can barely use the spatial unitary conditions (73) and (74) at all, because the operators following right on top of each other overlap on two sites, rather than one as for the time-evolution (87). So this time-evolution does not get us anywhere. In fact is also true for any other combination of all four operators. Thus the class of time-evolutions which include all four operators \mathbb{U}_{ee} , \mathbb{U}_{oo} , \mathbb{U}_{oe} and \mathbb{U}_{eo} is not useful to get exact results using ternary unitary operators.

The other class of time-evolutions contains time-evolutions of the form

$$\mathbb{U}_n = \mathbb{U}_{j_1 j_2} \mathbb{U}_{i_1 i_2}, \quad (131)$$

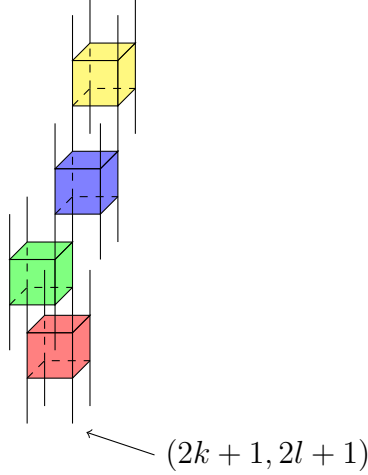


Figure 5: The time-evolution \mathbb{U}_{all} on a 3×3 -grid. Only the operators applied to sites that are all inside the grid are shown to avoid cluttering. The different operators are applied counter-clockwise around the middle site, which has odd-odd coordinates $(2k+1, 2l+1)$ with $k, l \in \mathbb{N}_0$. The different colours denote different gates, to distinguish which sites they are applied to.

where $i_1, i_2, j_1, j_2 \in \{e, o\}$ and $(i_1 = j_1) \leftrightarrow (i_2 = j_2)$. Let ι be the index for which $i_\iota = j_\iota$ and η the other one. This time-evolution (131) cannot be gained from H_{nn} via a Trotterisation of nearest-neighbour interactions, since we do not allow all nearest neighbours to interact. However, it is still interesting as it is simple to solve the correlation function exactly. A visualisation for one time-step and $(i_1, i_2, j_1, j_2) = (e, e, o, e)$ is given in Fig. 6. This kind of time-evolution consists of walls made of operators that stretch in direction e_ι over the entire grid-size and have a thickness of two sites in direction e_η . These walls are applied on two rows of sites, where one row of sites means the set of all sites that have the same e_η -coordinate. We call the union of two neighbouring rows that are connected by operators a *ribbon* of sites. The different walls are not connected to each other and therefore do not interact. A correlation function can be defined analogously to (88) as

$$D^{\alpha\beta}(x, y, t) = \frac{1}{d^{4L^2}} \text{Tr} [a_x^\alpha \mathbb{U}_n^{-t} a_y^\alpha \mathbb{U}_n^t]. \quad (132)$$

Clearly it will only be non-zero if x and y lie in the same ribbon. In this case walls applied to ribbons that do not entail x and y will immediately cancel with their hermitian conjugate via the unitary condition in time (72). What remains is a single wall for which we can just recycle the results from section 4.2. We define a new local Hilbert space $\tilde{\mathcal{H}}_{\text{loc}} = \mathcal{H}_{\text{loc}}^{\otimes 2}$ and new coordinates $\tilde{x} = x_\iota$ and $\tilde{y} = y_\iota$. Thus one site of the chain is made up of the two sites neighbouring each other along the e_η -direction in the ribbon. For these results to happen, we actually do not require our operators to be ternary unitary. It is sufficient for them to be unitary along the e_ι -direction. Therefore this is a special case of the time-evolution analysed in [13].

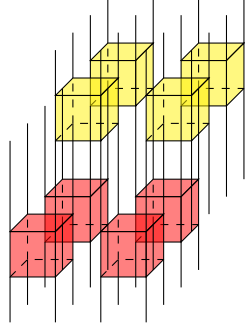


Figure 6: A visual representation of \mathbb{U}_n for $(i_1, i_2, j_1, j_2) = (e, e, o, e)$ and one time-step on a 4×4 -grid with periodic boundary conditions. \mathbb{U}_{ee} is represented by red and \mathbb{U}_{oe} by yellow cubes.

Now we know what characteristics are required for a time-evolution to be useful in $(2 + 1)$ -dimensional space-time. This will help us to define the correct evolution for an even greater number of spatial dimensions.

6 Extension to an arbitrary Number of spatial Dimensions

6.1 Definition and Correlation Functions

We defined a special class of unitary operators for one and two dimensions called dual unitaries and ternary unitaries respectively. They allowed for exact results and a lot of the arguments for one dimension were easily adaptable to two dimensions. Therefore analysing an analogous problem in even higher dimensional space-time can be considered a reasonable next step. While 3D-lattices are quite standard [14], higher dimensional lattices seem abstract at first and their usefulness is not obvious. However, 4D-lattices were found useful analysing a kind of quantum Hall effect [15]. Thus it seems worthwhile to take a chance at getting results for high dimensional lattices. For the definitions of the unusual high-dimensional geometric figures one can take a look at [16].

Let $\{e_i | i \in I_1(\Delta)\}$ be an orthonormal basis of \mathbb{R}^Δ . We can then define an evenly spaced Δ -dimensional lattice with all sides made up of $2L$ -sites as

$$\left\{ x = \sum_{j=1}^{\Delta} x_j e_j \mid x_j \in I_0(2L - 1) \forall j \right\} \simeq I_0(2L - 1)^\Delta. \quad (133)$$

Now associate to each site the d -dimensional Hilbert space $\mathcal{H}_{\text{loc}} = \mathcal{H}_x$ and denote its basis at site x as $B_x = \{|r\rangle_x \mid r \in I_0(d - 1)\}$. Let $U \in \text{End}(\mathcal{H}_{\text{loc}}^{\otimes 2^\Delta})$. It acts on 2^Δ -many

sites. We want it to more specifically act on the vertices of a Δ -dimensional hypercube, which would correspond to the Δ -dimensional lattice $\{0, 1\}^\Delta$. On such a lattice we can enumerate the sites via the map

$$F : \{0, 1\}^\Delta \rightarrow I_0(2^\Delta - 1) \quad (134)$$

$$i = \sum_{j=1}^{\Delta} 2^j x_j. \quad (135)$$

We will put the enumerating index upstairs x^i to avoid confusion with the element of the vector x_j . We can then describe the elements of U via

$$U_r^\rho = \left(\bigotimes_{x \in \{0,1\}^\Delta} \langle \rho_{F(x)} | \right) U \left(\bigotimes_{x \in \{0,1\}^\Delta} | r_{F(x)} \rangle \right), \quad (136)$$

where $|\rho_{F(x)}\rangle, |r_{F(x)}\rangle \in B_x$ and $r = (r_1, \dots, r_{2^\Delta-1})$, $\rho = (\rho_1, \dots, \rho_{2^\Delta-1})$. Before getting into the main definition, let us define the set

$$A_j = \{x \in \{0, 1\}^\Delta \mid x_j = 0\}. \quad (137)$$

This set includes all sites on a certain face of our hypercube. To be more precise, of the two faces orthogonal to e_j , it is the one closer to the origin.

Def. 3. An operator $U \in \text{End}(\mathcal{H}^{\otimes 2\Delta})$ is called a $(\Delta + 1)$ -**unitary** if it is unitary and for all $j \in I_1(\Delta)$ the operator U_j , defined via

$$\left(\bigotimes_{x \in A_j} \langle \rho_{F(x)} | \langle r_{F(x)} | \right) U_j \left(\bigotimes_{x \in \{0,1\}^\Delta \setminus A_j} | r_{F(x)} \rangle | \rho_{F(x)} \rangle \right) = U_a^\alpha, \quad (138)$$

is unitary, i.e.

$$U_j U_j^\dagger = \mathbb{1} \quad (139)$$

for all $j \in I_1(\Delta)$.

The demanded unitary conditions (139) are precisely the unitary conditions in the space directions. By defining a Δ -dimensional hyperplaquette as

$$P(x) = \left\{ z \in I_0(2L - 1)^\Delta \mid z = x + \sum_{j=1}^{\Delta} k_j e_j \quad \text{for } k \in \{0, 1\}^\Delta \right\}, \quad (140)$$

we can define the operators

$$U_e = \bigotimes_{\alpha \in I_0(L-1)^\Delta} I_{P(2\alpha)} \quad (141)$$

$$U_o = \bigotimes_{\alpha \in I_0(L-1)^\Delta} I_{P(2\alpha+1)}, \quad (142)$$

where $2\alpha + 1 = \sum_{j \in I_1(\Delta)} (2\alpha_j + 1) e_j$. This is from now on implied, whenever we add 1 to a vector. We once more assumed periodic boundary conditions. Now one step of the time-evolution is defined as

$$\mathbb{U}_\Delta = \mathbb{U}_o \mathbb{U}_e. \quad (143)$$

From the results in the previous section 5.3 we can conclude that our time-evolution should fulfil two properties:

1. After one time step, so one application of \mathbb{U}_Δ , every site should be connected to all of its neighbours via an operator.
2. An operator applied at a time τ should be connected to an operator at time $\tau \pm 1/2$ only via one event.

We can make these statements more rigorous:

1. For every pair of nearest neighbours $y \sim z$ there should be a site x with either all even or all odd coordinates, such that y, z are both in the hyperplaquette $P(x)$ defined by x , i.e. for all $(y \sim z)$

$$\exists x \in (\{2\alpha \mid \alpha \in I_0(L-1)^\Delta\} \cup \{2\alpha + 1 \mid \alpha \in I_0(L-1)^\Delta\}) : y, z \in P(x). \quad (144)$$

2. For operators following one another, one is applied to a hyperplaquette defined by a site with all even coordinates and the other by one with all odd coordinates. Therefore the desired property will be fulfilled if

$$|P(2\alpha) \cap P(2\beta + 1)| \in \{0, 1\} \quad \text{for all } \alpha, \beta \in I_0(L-1)^\Delta. \quad (145)$$

Proof. (1) Let $y \in I_0(2L-1)^\Delta$ be some site in our lattice. Its set of nearest neighbours is given by

$$N(y) = \left\{ y + (-1)^k e_j \mid j \in I_1(\Delta), k \in \{0, 1\} \right\}. \quad (146)$$

Also

$$\bigcup_{\alpha \in I_0(L-1)^\Delta} P(2\alpha) = \bigcup_{\beta \in I_0(L-1)^\Delta} P(2\beta + 1) = I_0(L-1)^\Delta \quad (147)$$

implies

$$\exists \alpha, \beta : y \in P(2\alpha) \quad \text{and} \quad y \in P(2\beta + 1). \quad (148)$$

Now we can look in each spatial dimension at two different cases.

First, we assume y_j is even. Then (148) and the definition of a hyperplaquette (140) imply

$$y_j = (2\alpha)_j \quad (149)$$

$$y_j = (2\beta + 1)_j + 1. \quad (150)$$

This in turn implies that

$$y + e_j \in P(2\alpha) \quad (151)$$

$$y - e_j \in P(2\beta + 1). \quad (152)$$

In a similar way we get that for odd y_j

$$y - e_j \in P(2\alpha) \quad (153)$$

$$y + e_j \in P(2\beta + 1). \quad (154)$$

Since this is true for all j we get

$$N(y) \subset P(2\alpha) \cup P(2\beta + 1). \quad (155)$$

□

Proof. (2) It is immediately clear that the overlap is empty for

$$\|2\alpha - (2\beta + 1)\|_\infty > 1 \quad (156)$$

and, since $2\alpha \neq 2\beta + 1$, the statement has to be shown only for

$$\|2\alpha - (2\beta + 1)\|_\infty = 1. \quad (157)$$

This immediately implies

$$|(2\alpha)_j - (2\beta + 1)_j| = 1 \quad \forall j \in I_0(\Delta) \quad (158)$$

$$\Rightarrow \quad 2\beta + 1 = 2\alpha + \sum_{j=1}^{\Delta} k_j e_j \quad \text{for some } k \in \{-1, 1\}^\Delta \quad (159)$$

$$\Rightarrow \quad P(2\beta + 1) = \left\{ z \mid z = 2\alpha + \sum_{j=1}^{\Delta} (k_j + l_j) e_j \quad \text{with } l \in \{0, 1\}^\Delta \right\}. \quad (160)$$

On the other hand

$$P(2\alpha) = \left\{ z \mid z = 2\alpha + \sum_j \tilde{l}_j e_j \quad \text{with } \tilde{l} \in \{0, 1\}^\Delta \right\}. \quad (161)$$

Therefore, $z \in P(2\beta + 1) \cap P(2\alpha)$ if and only if

$$k + l \in \{0, 1\}^\Delta \quad (162)$$

$$\Leftrightarrow k_j + l_j \in \{0, 1\}. \quad (163)$$

Thus if $z \in P(2\alpha) \cap P(2\beta + 1)$

$$\begin{aligned} k_j = 1 &\Rightarrow l_j = 0 \\ k_j = -1 &\Rightarrow l_j = 1. \end{aligned} \quad (164)$$

As k is fixed by α and β , such an l will be unique, proving the claim. □

Now that this is done we can compute the correlation function

$$D^{\alpha\beta}(x, y, t) = \frac{1}{d^{(2L)\Delta}} \text{Tr} [a_x^\alpha \mathbb{U}_\Delta^{-t} a_y^\alpha \mathbb{U}_\Delta^t]. \quad (165)$$

By once more using the trick of choosing $\{a_x^\alpha\}_{\alpha \in I_0(d^2-1)}$ as a basis of local operators on \mathcal{H}_x and choosing $a_x^0 = \mathbb{1}$ and $\text{Tr} [a_x^\alpha a_x^\beta] = d\delta_{\alpha\beta}$, we get again equation (89) which implies (90). So we may assume $\alpha \neq 0$ and $\beta \neq 0$. In a similar fashion as before we can get a light-cone, due to the unitary condition in time and the properties (144) and (145), as follows

$$\mathcal{LC} = \left\{ (z, \tau) \in I_0(2L-1)^\Delta \times I_0(2t-1)/2 \mid \min_{\tilde{y} \in P_m} \|z - \tilde{y}\|_\infty \leq 2t - 1 - 2\tau \right\}, \quad (166)$$

where $P_m = P(2\lceil \frac{y}{2} \rceil - 1)$. \mathcal{LC} looks like a Δ -dimensional hyperpyramid. Using the unitary property in time for all operators not applied to events in \mathcal{LC} the trace in (165) reduces to

$$\text{Tr} [a_x^\alpha \mathbb{U}_\Delta^{-t} |_{\mathcal{LC}'} a_y^\alpha \mathbb{U}_\Delta^t |_{\mathcal{LC}}], \quad (167)$$

where

$$\mathcal{LC}' = \left\{ (z, \tau) \in I_0(2L-1)^\Delta \times I_t(2t-1)/2 \mid \min_{\tilde{y} \in P_m} \|z - \tilde{y}\|_\infty \leq 2\tau - 2t \right\}. \quad (168)$$

So the events on which the hermitian conjugate operators are applied are associated with the times $\tau \in I_t(2t-1)/2$, i.e. we just continue counting in time direction even after reaching $\tau = t$.

We can enumerate the sites in P_m , for example via

$$\begin{aligned} \tilde{F} : P_m &\rightarrow I_0(2^\Delta - 1) \\ \tilde{y} &\mapsto i = F(\tilde{y} - (2\lceil y/2 \rceil - 1)). \end{aligned} \quad (169)$$

Again we will put this enumeration index upstairs. Now we may define different boundary hypersurfaces of the light-cone $\mathcal{LC}(\tau)$ at a time τ as

$$S^i(\tau) = \{z \in \mathcal{LC}(\tau) \mid \|z - y^{i_k}\|_\infty = 2t - 2\tau \ \forall k \in I_1(2\Delta)\}, \quad (170)$$

where $i \in (I_0(2^\Delta - 1) \setminus (i_k = i_{k'}))$ and $(i_k = i_{k'})$ denotes the set of $i \in I_0(2^\Delta - 1)$ such that there exist $k \neq k'$ with $i_k = i_{k'}$. Note that $S^i(0)$ are the sides of the base of our hyperpyramid.

Now we have to distinguish cases in a similar manner as we did in the sections with low-dimensional space-time. Let $y = y^t \in P_m$ with $\iota \in \tilde{F}(P_m)$ fixed and assume that

$$x \notin \bigcap_{\iota \in i} S^i(0) \quad (171)$$

i.e., x does not fulfil

$$|x_j - y_j| = 2t \quad \forall j \in I_1(\Delta). \quad (172)$$

Thus there exists i such that $x \notin S^i(0)$ and $\iota \in i$. Also assume the lattice size to fulfil $L \geq 2t$. One more thing to define is

$$\mathfrak{U}^i(\tau) = \{U_{(P(U),\tau)} \mid P(U) \cap S^i(\tau) \neq \emptyset\}. \quad (173)$$

What comes next is not at all trivial, since we are missing any kind of visualisation. However, if one gets stuck it helps to compare the following to the corresponding part of section 5.2, since the fundamental ideas are the same.

By definition we know

$$\mathcal{LC} \left(\tau + \frac{1}{2} \right) \cap S^i(\tau) = \emptyset \quad (174)$$

$$\mathcal{LC}' \left(2t - \tau - \frac{1}{2} \right) \cap S^i(\tau) = \emptyset \quad (175)$$

for all $\tau \in I_0(t-1)$. This implies that events of the form $(z, \tau + 1/2)$ with $z \in S^i(\tau)$ are connected to events $(z, 2t - \tau - 1/2)$ via the identity. Now assume that (z, τ) with $z \in S^i(\tau)$ are all connected to the events $(z, 2t - \tau)$ via the identity. Take some $z' \in S^i(\tau)$ and define the normalised vector e_j as perpendicular to $z' - z$ for all $z \in S^i(\tau)$ and $e_j \cdot (y - z') > 0$. Basically it should point from the side $S^i(\tau)$ towards the center of the light-cone. The connections between certain events allow us to apply the unitary condition in the direction e_j to all $U_{(P(U),\tau)} \in \mathfrak{U}^i(\tau)$ and their conjugate counterparts. This leads to $(z + e_j, \tau + 1/2)$ being connected to $(z + e_j, 2t - \tau - 1/2)$. As $z + e_j \in S^i(\tau + 1/2)$, we can apply the same reasoning again for operators $U_{(P(U),\tau+1/2)} \in \mathfrak{U}(\tau + 1/2)$. There is a suitable base case for this recursion: By definition of the trace, $(z, 0)$ for $z \in S^i$ is connected to $(z, 2t)$ via the identity. Thus we can iterate the argument $(2t-1)$ -times starting from $\tau = 0$. We have to stop at $\tau = t-1$, since $\mathcal{LC}(t)$ is not defined, so (175) would be ill-defined. But that is still sufficient to find that every event $(z, t-1/2)$ with $z \in S^i(t-1)$ is connected to the event $(z, t+1/2)$ via the identity. As $z \in S^i \subset P_m$ and $y \notin S^i(t-1/2)$ by assumption, only the identity acts on sites (z, t) before $U_{P_m}^\dagger$ acts on them. Thus we can apply the unitary condition in the e_j direction one last time causing events (z, t) with $z \in P_m \setminus S^i(t-1/2)$ to be connected to themselves. One of these events is (y, t) , on which a_y^β acts. This implies

$$D^{\alpha\beta} \propto \text{Tr} [a_y^\beta] = 0. \quad (176)$$

Now assume x fulfils (172). This implies that we cannot find i such that $x \notin S^i$, which is required for the base case to be true, and $\iota \in i$, which is required for the last application of the unitary condition. But we know the position of x relative to y which allows us to find \mathcal{C} as defined in (104). With the same arguments as in section 5.2

but extended to Δ dimensions, we can break that computation down to handle each dimension independently. By using the results gained in section 4.2, we get

$$\mathcal{C} = \left\{ (z, \tau) \in \bigotimes_{j=1}^{\Delta} R_j(I_0(2L-1)) \times I_0(2t-1)/2 \mid z = x + \sum_{j=1}^{\Delta} 2\tau e_j \right\}. \quad (177)$$

Thus what remains after applying all possible unitary conditions in time is a string of operators that are applied to the events in \mathcal{C} .

We can once more define a new operator to make the result more precise. Let there be a Δ -dimensional lattice of size 2 on which we define the new operator

$$M(a, y) = \frac{1}{d^{2\Delta-1}} \text{Tr}_{\{0,1\}^{\Delta} \setminus \{0\}} [\mathcal{S}^\dagger(y) U^\dagger \mathcal{S}^\dagger(y) \tilde{a} \mathcal{S}(y) U \mathcal{S}(y)], \quad (178)$$

where 0 is the zero-vector and $\tilde{a} = \bigotimes_{i \in \{0,1\}^{\Delta}} \left(\delta^{i, \tilde{1}} a_{\tilde{1}} + (1 - \delta^{i, \tilde{1}}) \mathbb{1}_i \right)$, with $\tilde{1} = \sum_{j=1}^{\Delta} e_j$. Which means a is always applied at site $\tilde{1}$ and to the remaining sites the identity is applied. Furthermore we define

$$\mathcal{S}(y) = \prod_{j=1}^{\Delta} \left(\bigotimes_{\substack{i \in \{0,1\}^{\Delta} \\ : i_j=0}} \text{SWAP}_{(\sum_{k=1}^{\Delta} i_k e_k, \sum_{k=1}^{\Delta} i_k e_k + e_j)} \right)^{y_j}. \quad (179)$$

Both are just generalised versions of their counterparts in section 5.2. We can then write the correlation function as

$$D^{\alpha\beta}(x, y, t) = \frac{1}{d} \text{Tr} [M^{2t}(a_y^\beta, y) a_x^\alpha], \quad (180)$$

which is exactly the same as (118). Basically copying (119), we can summarize our results as

$$D^{\alpha\beta}(x, y, t) = \begin{cases} \delta_{0\beta} & \text{if } \alpha = 0 \\ \delta_{\alpha 0} & \text{if } \beta = 0 \\ 0 & \text{if } x \neq y + \sum_{i=1}^{\Delta} (-1)^{y_i+1} t e_i \text{ and } \alpha, \beta \neq 0 \\ \frac{1}{d} \text{Tr} [M^{2t}(a_y^\beta, y) a_x^\alpha] & \text{if } x = y + \sum_{i=1}^{\Delta} (-1)^{y_i+1} t e_i \text{ and } \alpha, \beta \neq 0 \end{cases}. \quad (181)$$

6.2 Properties of the M-Map

In equation (178) and during the earlier sections, we introduced the operator valued maps $M_y(a) = M(a, y)$. To be more precise

$$M_y : \text{End}(\mathcal{H}_{\text{loc}}) \rightarrow \text{End}(\mathcal{H}_{\text{loc}}). \quad (182)$$

In this section we want to proof properties that were stated in [1] for one spatial dimension for general M -maps. First we require the two definitions

Def. 4. Let \mathcal{H}_{loc} be a finite d -dimensional Hilbert space. A map $\Phi : \text{End}(\mathcal{H}_{loc}) \rightarrow \text{End}(\mathcal{H}_{loc})$ is called **k -unistochastic** [17] if there exists a unitary matrix $U \in \text{End}(\mathcal{H}_{loc} \otimes \mathcal{H}_{env})$ for some additional finite (dk) -dimensional Hilbert space \mathcal{H}_{env} such that

$$\Phi(\rho) = \frac{1}{dk} \text{Tr}_{env}[U^\dagger(\rho \otimes \mathbb{1})U] \quad , \quad (183)$$

where $k \in \mathbb{N}$.

Def. 5. Let \mathcal{H} be a finite dimensional Hilbert space. A map Φ over $\text{End}(\mathcal{H})$ is called **bistochastic** [18] if it is completely positive, trace preserving and unital, i.e. the identity is an eigenvector of Φ with eigenvalue $\lambda = 1$.

Property 2. M_y is $d^{2^\Delta-2}$ -unistochastic and linear for all $y \in \mathbb{Z}^\Delta$.

Proof. By rewriting

$$\begin{aligned} \mathcal{H}_{env} &= \prod_{i \in \{0,1\}^\Delta \setminus \{0\}} \mathcal{H}_i = \mathcal{H}_{loc}^{\otimes (2^\Delta-1)} \\ k &= d^{2^\Delta-2} \\ U' &= \mathcal{S}(y)U\mathcal{S}(y) \\ \rho &= a \end{aligned}$$

and inserting this into the definition (178) of M_y , M_y will be of the form (183) and thus $d^{2^\Delta-2}$ -unistochastic. Clearly the linearity of M_y follows from its $d^{2^\Delta-2}$ -unistochasticity. \square

Lemma 1. Every k -unistochastic map is bistochastic.

Proof. Let Φ be a k -unistochastic map and $\{|i\rangle\}_{i=0}^{dk-1}$ a basis of \mathcal{H}_{env} . We can rewrite (183) as

$$\Phi(\rho) = \frac{1}{dk} \sum_i \langle i|U^\dagger(\rho \otimes \mathbb{1})U|i\rangle. \quad (184)$$

As ρ being positive implies $(\rho \otimes \mathbb{1})$ being positive and every map Φ' of the form

$$\Phi'(\rho) = \sum_i V_i^\dagger \rho V_i \quad (185)$$

is completely positive [19], Φ is completely positive. As U is unitary, Φ is trace preserving,

$$\text{Tr}_{loc}[\Phi(\rho)] = \frac{1}{dk} \text{Tr}[(\rho \otimes \mathbb{1})UU^\dagger] = \frac{1}{dk} \text{Tr}[(\rho \otimes \mathbb{1})] = \text{Tr}_{loc}[\rho] \quad (186)$$

and unital

$$\Phi(\mathbb{1}) = \frac{1}{dk} \text{Tr}_{env}[U^\dagger U] = \mathbb{1}. \quad (187)$$

\square

Using Lemma 1 we get

Property 3. M_y is bistochastic for all $y \in \mathbb{Z}^\Delta$.

Property 4. The maps M_y have a spectrum that lies on the complex unit disk and all eigenvalues on the unit circle have coinciding algebraic and geometric multiplicity.

Proof. The proof given in [1] was done for the maps M_y with $y \in \{0, 1\}$ in $(1 + 1)$ -dimensional space-time which are given in (60). That proof trivially extends to our bistochastic M_y -maps for an arbitrary number of space-dimensions. \square

We can now utilise the property 4:

First, we rewrite the trace in the final case of (181) as

$$\mathrm{Tr} [M_y^{2t} a_y^\beta a_x^\alpha] = \sum_{i,j=0}^{d-1} \langle i | M_y^{2t} (a_y^\beta) | j \rangle \langle j | a_x^\alpha | i \rangle. \quad (188)$$

Now we may reinterpret the operator a_y^β as a vector and M_y as matrix. We can then bring M_y into Jordan normal form and denote the eigenvalues as $\{\lambda_{\nu,y}\}_{\nu=0}^{d^2-1}$. If an eigenvalue $\lambda_{\nu,y}$ is not on the unit disk, its Jordan block $J_{\nu,y}$ will give rise to a block in M_y^{2t} of the form

$$J_{\nu,y}^{2t} = \begin{pmatrix} \lambda_{\nu,y}^{2t} & \binom{2t}{1} \lambda_{\nu,y}^{2t-1} & \dots & \binom{2t}{n} \lambda_{\nu,y}^{2t-n} \\ 0 & \lambda_{\nu,y}^{2t} & \dots & \binom{2t}{n-1} \lambda_{\nu,y}^{2t-n+1} \\ \vdots & \vdots & \ddots & \vdots \\ 0 & 0 & \dots & \lambda_{\nu,y}^{2t} \end{pmatrix}, \quad (189)$$

where n is the size of the original Jordan block $J_{\nu,y}$ [20]. On the other hand, if $\lambda_{\nu,y}$ is on the unit circle, the corresponding block of size 1 is given by $\lambda_{\nu,y}^{2t}$.

Now we may perform the multiplication $M_y^{2t} \cdot a_y^\beta$ in matrix/vector-representation. Inserting the resulting vector back into the trace in (188), we get

$$\mathrm{Tr} [M_y^{2t} (a_y^\beta) a_x^\alpha] = \sum_{\nu=1}^{d^2-1} c_{\nu,y}^{\alpha\beta}(t) \lambda_{\nu,y}^{2t}, \quad (190)$$

where the trivial eigenvalue for the eigenvector $\mathbb{1}$ corresponding to $\nu = 0$ is already left out, since we assumed $\mathbb{1}$ to be orthogonal to a_y^β . In order to get the factor $\lambda_{\nu,y}^{2t}$ for each term, some powers of $\lambda_{\nu,y}$ are absorbed into the coefficient $c_{\nu,y}^{\alpha\beta}(t)$, which will be a polynomial in t . This is the same final result as in [1] for one spatial dimension and we could use it to simplify rewrite the last case of the correlation function given in (181). We could now find a classification by ergodicity for all $(\Delta + 1)$ -unitaries, using the eigenvalues $\lambda_{\nu,y}$. The classes would be precisely the same as in [1], so the classification will be omitted here.

6.3 Examples of the M-Map

We can take some of the examples of $(\Delta + 1)$ -unitaries to construct examples of M -maps.

6.3.1 (1+1)-dimensional Lattices

We start with a little warm-up and use the **SWAP** as the dual-unitary to construct M . We get

$$M(2l, a) = \frac{1}{d} \left[\text{Diagram: A vertical line with a dot labeled 'a' in the middle. To its left, two lines cross twice, forming a hexagonal shape that encloses the dot. The top and bottom lines of this hexagon extend to the left and right edges of the diagram. To the right of the dot, a vertical line extends from the top to the bottom of the hexagon. This entire structure is enclosed in a larger vertical frame.] = \bullet a \cdot \quad (191)$$

Clearly $M(2l, a) = M(2l + 1, a) = a$, so $M = \mathbb{1}$. A more intricate example can be found when restricting to $d = 2$ and using the parametrisation (28) of \mathcal{DU} . In [1] it was found using $\{a^0, a^1, a^2, a^3\} = \{\mathbb{1}, \sigma^x, \sigma^y, \sigma^z\}$ as a base, that M -maps take the form

$$M_{2l} = \begin{pmatrix} 1 & 0 \\ 0 & R[u_-] \end{pmatrix} \text{diag}[1, \sin(2J), \sin(2J), 1] \begin{pmatrix} 1 & 0 \\ 0 & R[v_-] \end{pmatrix}, \quad (192)$$

where $R[w]$ is the adjoint representation of $SU(2)$ defined by

$$R[w]_{(\alpha, \beta)} = \frac{1}{2} \text{Tr} [\sigma^\alpha w \sigma^\beta w^{-1}]. \quad (193)$$

For M_{2l+1} we need only replace $- \rightarrow +$.

6.3.2 (2+1)-dimensional Lattices

For the $(2 + 1)$ -dimensional space-time, we had a class of ternary unitaries described in (77) and (78). We can now compute an example of M being constructed by $X(U, V, W, T)$. We use a visualisation to aid us:

$$M(a) = \frac{1}{d^3} \left[\text{Diagram: A 3D lattice structure with four vertical lines. The top two lines are labeled U* and V*. The bottom two lines are labeled W and T. There are blue shaded regions between U* and V*, and between W and T. There are red shaded regions between U* and W, and between V* and T. A dot labeled 'a' is on the right line. The diagram is enclosed in a 3D frame.] = \frac{1}{d^2} \left[\text{Diagram: A 2D lattice structure with two vertical lines. The top line is labeled V* and the bottom line is labeled T. There is a blue shaded region between V* and T. A dot labeled 'a' is on the right line.] = \frac{1}{d^2} \left[\text{Diagram: A 2D lattice structure with two vertical lines. The top line is labeled V* and the bottom line is labeled U. There is a blue shaded region between V* and U. A dot labeled 'a' is on the right line.] \cdot \quad (194)$$

In the first equality we used both the usual (22) and dual unitary condition (23) and in the second one we merely readjusted the tensors. By enumerating the three sites from left to right as 1, 2, 3 we get

$$\begin{aligned} M(a) &= \text{Tr}_1 \left[U_{(1,2)}^\dagger \text{Tr}_3 \left[\left(\mathbb{1}_1 \otimes V_{(2,3)}^\dagger \right) \left(\mathbb{1}_1 \otimes \mathbb{1}_2 \otimes a \right) \left(\mathbb{1}_1 \otimes V_{(2,3)} \right) \right] U_{(2,3)} \right] \\ &= \hat{M}_2[U] \left(\hat{M}_2[V](a) \right), \end{aligned} \quad (195)$$

where $\hat{M}_2[U]$ denotes the M_2 -operator of the $(1 + 1)$ -dimensional lattice that is constructed from $U \in \mathcal{DU}(d)$. Clearly the maps for different positions of a and the construction Y instead of X would lead to a similar result.

Thus we see that by constructing the ternary unitaries via the lower dimensional dual unitaries, the resulting M -maps can also be constructed, using the lower dimensional \hat{M} -maps.

7 Unitaries and Index Permutations

We established dual-, ternary- and general $(\Delta + 1)$ -unitaries and obtained exact results. However, examples of $(\Delta + 1)$ -unitaries in particular for high dimensions either in space or of \mathcal{H}_{loc} are few. We can find some by connecting the $(\Delta + 1)$ -unitaries with other classes of unitary operators that were already established in the literature.

Let us start by breaking down the definitions (1), (2) and (3) used in the previous sections. We defined dual-, ternary- and general $(\Delta + 1)$ -dimensional unitaries by interpreting them as tensors and demand certain unitary conditions. For that we split their tensor indices \mathcal{A} into two sets A and \tilde{A} and viewed the tensors as matrices with A and \tilde{A} defining one index of the matrix each. The two sets were chosen such that the matrix multiplication would be along a certain space-time direction. Clearly one could define other sets of matrices by splitting the tensor indices in different ways and demanding the resulting matrices to be unitary. We will find that some of these classes have surprising properties and applications. But first we need to introduce some notation:

Def. 6. Let T be an n -tensor, $K = \{k_1, \dots, k_n\}$ the set of indices of T , and \mathcal{H}_{k_i} the d_i -dimensional Hilbert space associated to index k_i with basis $\{|k_i\rangle\}_{k_i=0}^{d_i-1}$. For $\pi \in \sigma(I_1(n))$ and $s \in I_1(n-1)$, define the (π, s) -**matrix** \tilde{T} of T via

$$\tilde{T}_{[k_{\pi(1)}, \dots, k_{\pi(s)}], [k_{\pi(s+1)}, \dots, k_{\pi(n)}]} = \langle k_{\pi(1)}, \dots, k_{\pi(s)} | \tilde{T} | k_{\pi(s+1)}, \dots, k_{\pi(n)} \rangle = T_{k_1, \dots, k_n}. \quad (196)$$

Sometimes we explicitly write $\tilde{T}_{(\pi, s)}$.

While this notion is very general it is frequently used albeit implicit. One such use is in combination with the singular value decomposition (SVD) that allows to split tensors into a tensor network:

$$T_{k_1, \dots, k_n} = \sum_{i, j} U_{k_{\pi(1)}, \dots, k_{\pi(s)}, i} S_j^i (V^\dagger)_{k_{\pi(s+1)}, \dots, k_{\pi(n)}}^j, \quad (197)$$

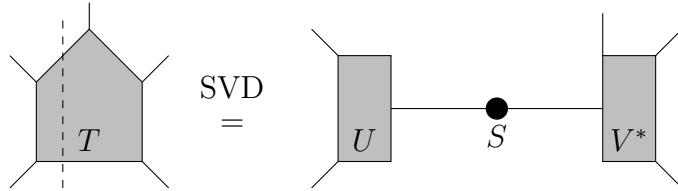


Figure 7: The tensor network that results from applying the SVD on a 5-tensor T . The dashed line shows where we want to "cut" with the SVD. It is a visual representation of our choice of (π, s) .

where U , S , and V are the tensors that we get by reorganising the matrices that make up the SVD of the matrix-representation $\tilde{T}_{\pi,s}$ of T . A visual example for $n = 5$ is given in Fig. 7. The SVD is usually used to allow for useful properties or simplifications later on. Examples of the procedure include but are in no way limited to the canonical forms of matrix product states [8], the time-evolution of such states via the iTEBD algorithm [21] and methods to get efficient algorithms for 2D systems [22, 23]. Going into detail on each would go beyond the scope of this thesis. Instead we will proceed along this section's motivation and define sets of tensors by properties of their matrix representations.

We start with the most general definition, which is the notion of perfect tensors introduced in [24]:

Def. 7. Let T be an n -tensor with all local dimensions being equal to d and the index set $K = \{k_1, \dots, k_n\}$. T is called a **perfect tensor** [24] if for all $\pi \in \sigma(I_1(n))$ and s with $2s \leq n$

$$\tilde{T}_{(\pi,s)} \left(\tilde{T}_{(\pi,s)} \right)^\dagger = \mathbb{1}. \quad (198)$$

We have to restrict the choice of s , since $\tilde{T}_{(\pi,s)}$ is a $d^s \times d^{n-s}$ -sized matrix. If $d^s \geq d^{n-s}$, equation (198) could not be fulfilled and the definition would be useless. In [24] it was found that perfect tensors give rise to quantum error correcting codes (QECC). The specific set arising in such a way are called holographic QECCs. These in turn can be used to study the AdS/CFT correspondence, where the holographic QECCs can be used as toy models [24]. Once more the details would go beyond the scope of this thesis. Nevertheless it is worthwhile to look at another nice detail that we can connect to dual unitaries in the later parts of this section.

It was shown that demanding fewer of the unitary constraints (198) still allows for holographic QECCs [25]. Thus we might look at all tensors T which fulfil (198) for all cyclic permutations π , but are not required to do so for other permutations. Such tensors are called **block perfect tensors**. Clearly every perfect tensor is a block perfect tensor. However, generally a block perfect tensor is not a $(\Delta+1)$ -unitaries, since some of the unitary conditions demanded in the definition (3) are not for cyclic matrix-representations of the tensor U .

We can use a different set of unitary conditions. We will find that the resulting class of unitary operators provides examples for $(\Delta + 1)$ -unitaries.

Def. 8. Let T be a $2n$ -tensor. We call T an n -**unitary** [26] if

$$T_{(\pi,n)} (T_{(\pi,n)})^\dagger = \mathbb{1} \quad (199)$$

for all $\pi \in \sigma(I_1(2n))$.

We basically demand the two sets of indices to have the same cardinality n and thus restrict s , rather than π as for the block perfect tensors. To see that they actually provide examples for $(\Delta + 1)$ -unitaries we must first proof the following:

Lemma 2. Let $\pi, \kappa \in \sigma(I_1(n))$ such that their images on $\{k_1, \dots, k_s\}$ are equal

$$\pi(\{k_1, \dots, k_s\}) = \kappa(\{k_1, \dots, k_s\}) \quad (200)$$

for some $s, n \in \mathbb{N}$ with $2s \leq n$. Then for T an n -tensor

$$T_{(\pi,s)}(T_{(\pi,s)})^\dagger = \mathbb{1} \quad \Rightarrow \quad T_{(\kappa,s)}(T_{(\kappa,s)})^\dagger = \mathbb{1}. \quad (201)$$

The same is true if π, κ are such that

$$\pi(\{k_{s+1}, \dots, k_n\}) = \kappa(\{k_{s+1}, \dots, k_n\}). \quad (202)$$

Proof. It is sufficient to show this for $[k_{\pi(1)}, \dots, k_{\pi(s)}]$ and $[k_{\kappa(1)}, \dots, k_{\kappa(s)}]$ differing by an elementary permutation only. Thus we can write

$$[k_{\kappa(1)}, \dots, k_{\kappa(j)}, \dots, k_{\kappa(i)}, \dots, k_{\kappa(s)}] = [k_{\pi(1)}, \dots, k_{\pi(i)}, \dots, k_{\pi(j)}, \dots, k_{\pi(s)}]. \quad (203)$$

This in turn implies

$$T_{(\kappa,s)} = T_{(\pi,s)} \mathbf{SWAP}_{(k_{\pi(i)}, k_{\pi(j)})}. \quad (204)$$

Which gives the desired result, if inserted in (201). The case for (202) follows immediately, since (200) is equivalent to (202). \square

Therefore, only the set of indices we choose to make up the row index of the resulting matrix matters for the unitary conditions. Thus we have only $N = \binom{2n}{n}$ independent conditions (199) for a tensor T to be a k -unitary. Basically we choose n different indices out of the total $2n$ indices to make up the row index of the resulting matrix. The number of independent unitary conditions is actually even lower, since for the square $n \times n$ -matrices $T_{(\pi,2)}$

$$T_{(\pi,2)}(T_{(\pi,2)})^\dagger = \mathbb{1} \quad \Rightarrow \quad (T_{(\pi,2)})^\dagger T_{(\pi,2)} = \mathbb{1}. \quad (205)$$

This further halves the number of unitary conditions for n -unitary tensors.

Lemma 2 is also important, since the same is true for the $(\Delta + 1)$ -unitaries: It only matters that we choose all the systems on one face of the hypercube, i.e. A defined in

(137), while the order of the tensor products in equation (138) does not matter. Thus we can connect the n -unitaries to the $(\Delta + 1)$ -unitaries by looking at the unitary conditions used in each definition. In Def. 3 of the $(\Delta + 1)$ -unitaries we demanded $(\Delta + 1)$ -many different matrix representations of a $2^{\Delta+1}$ -tensor U to be unitary. Each of these matrix representations corresponds to a $(\pi, 2^\Delta)$ -matrix of U , each for a different permutation $\pi \in \sigma(I_1(2^{\Delta+1}))$. Since

$$\Delta + 1 < \binom{2^{\Delta+1}}{2^\Delta} / 2 \quad (206)$$

for $\Delta \geq 1$, the number of unitary conditions in Def. 3 is less than in Def. 8 for a 2^Δ -unitary. As all unitary conditions required in Def. 3 are also demanded in Def. 8, any 2^Δ -unitary is a $(\Delta + 1)$ -unitary. As examples of the n -unitaries are known, especially by connecting them to maximally entangled states [26], we have also found examples of $(\Delta + 1)$ -unitaries.

We can find more relationships between the different classes of unitaries. While it is clear that any perfect $2n$ -tensor is an n -unitary and in turn any perfect $2^{\Delta+1}$ -tensor is a $(\Delta + 1)$ -unitary, this is not generally true for block perfect tensors of the same order. To be more precise, by looking at the different conditions demanded for each class, we can see that only in the case of $n = 2$ a block perfect $2n$ -tensor is always an n -unitary tensor. For $n > 2$ there is no relation between n -unitaries and block perfect $2n$ -tensors. However, we can combine the ideas of both definitions to get

Def. 9. *Let T be a $2n$ -tensor. It is called a **cyclic n -unitary** if for all cyclic permutations $\pi \in \sigma(I_1(2n))$*

$$T_{(\pi,n)}(T_{(\pi,n)})^\dagger = \mathbb{1}. \quad (207)$$

Clearly all n -unitaries and all block perfect $2n$ -tensors are cyclic n -unitaries. It turns out that for $n = 2$ the dual unitaries and for $n = 3$ the tri-unitaries introduced in [3] coincide with cyclic n -unitaries. Both act in only $(1 + 1)$ space-time dimensions. For the more general $(\Delta + 1)$ -unitaries such a fairly one-dimensional concept as the cyclicity seems insufficient for a classification. A visual summary of the relations established between the different classes of unitary tensors in this section is shown in Fig. 8. Now that the background and existence of examples for $(\Delta + 1)$ -unitaries has been established, we will find in the next section that actually using them for computations is not trivial. However, for simplicity we will do this for $(1 + 1)$ - and $(2 + 1)$ -dimensional space-times only.

8 Implementation on a Quantum Computer

8.1 Solvable initial States

Now after these quite abstract sections, let us consider some concepts closer to application. While dual unitaries seem to have some nice properties that allow for analytical results, it is still hard to actually compute dynamics for arbitrary initial states [6]. To

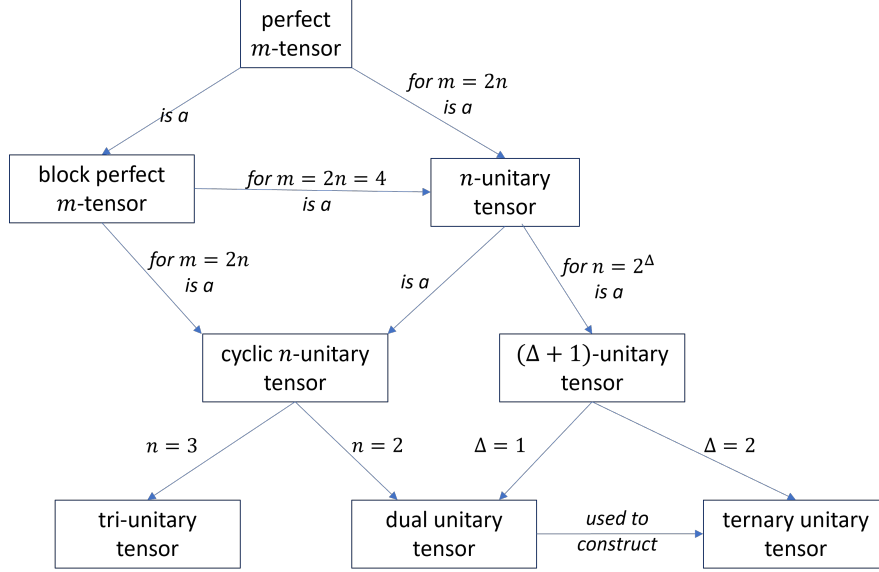


Figure 8: A visualisation of the different connections made in this section between different kinds of operator sets.

tackle this problem special so-called solvable states were introduced in [6]. They have to fulfil conditions that allow for an exact computation of the time-evolution of local observables, correlation functions and entropy of entanglement.

The property that is most important to us is that such states give rise to a tensor network with few traces that connect different times, but still allow for exact solutions. In this subsection we will define the solvable state and establish their basic properties. For that we once more study a chain of $2L$ sites, each associated to a local Hilbert space \mathcal{H}_{loc} of finite dimension d . On such a chain, a two-site shift-invariant state in the form of a matrix product state (MPS) [8] is given as

$$|\Psi^L(N)\rangle = \sum_{i_1, j_1, \dots, i_L, j_L=1}^d \text{Tr} [N^{i_1 j_1} \dots N^{i_L j_L}] |i_1, j_1 \dots i_L, j_L\rangle, \quad (208)$$

where $N^{(i,j)} \in \text{End}(\mathcal{H}_{\text{virt}})$ describes two systems at the same time and $\mathcal{H}_{\text{virt}}$ is a χ -dimensional Hilbert space. χ is called bond or virtual dimension. Furthermore, $|\Psi^L(N)\rangle$ is assumed to be normalised for all L . Like any other MPS these states can be represented by a tensor network diagram:

$$\text{Tr} [N^{i_1 j_1} \dots N^{i_L j_L}] = \text{Diagram}, \quad (209)$$

where the red legs correspond to the physical indices i_k, j_k . To continue we need to define

Def. 10. Two classes of two-site shift-invariant MPSs $\{|\Phi^L\rangle\}_L$ and $\{|\Psi^L\rangle\}_L$, defined on increasing system sizes L , are **equivalent** [6] if

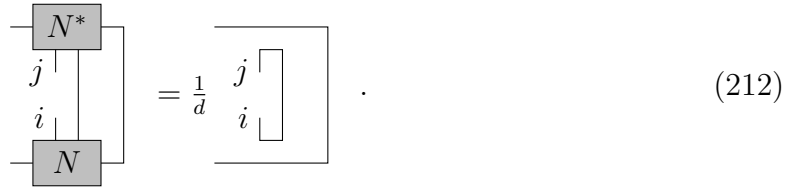
$$\lim_{L \rightarrow \infty} \langle \Phi^L | \mathcal{O}_R | \Phi^L \rangle = \lim_{L \rightarrow \infty} \langle \Psi^L | \mathcal{O}_R | \Psi^L \rangle \quad (210)$$

for all operators that are acting non-trivially only on a finite part of the system. In this case one might say that two states $|\Phi_0^L\rangle$ and $|\Psi_0^L\rangle$ are equivalent (in the thermodynamic limit).

In [6] it was shown that any solvable state is equivalent to a state $|\Psi_0^L(N)\rangle$ that is injective as defined in [27] with the operator N fulfilling

$$\sum_{k=0}^{d-1} N^{ik} (N^{jk})^\dagger = \frac{1}{d} \delta_{ij}, \quad (211)$$

which can be visualised as



$$\begin{array}{c} \boxed{N^*} \\ | \\ j \\ | \\ \boxed{N} \\ | \\ i \end{array} = \frac{1}{d} \boxed{\begin{array}{c} j \\ | \\ i \end{array}} . \quad (212)$$

Equation (211) implies

$$\sum_{k=1}^d (N^{ki})^\dagger N^{kj} = \frac{1}{d} \delta_{ij} \quad , \quad (213)$$

which can be visualised in a similar manner. Now, let $|\Psi_0^L(N)\rangle$ be an injective state fulfilling (211). It was found using (211), that such states can be parametrized using unitary operators $W \in \text{End}(\mathcal{H}_{\text{loc}} \otimes \mathcal{H}_{\text{virt}})$. In [6] such a parametrisation of a non-trivial for the example was found:

Example 5. Let bond dimension $\chi = 2$ and physical dimension $d = 2$, i.e. qubits. The four matrices N^{ij} from which we can create the desired injective states $|\Psi_0^L(N)\rangle$ fulfilling (211) can be parametrised as

$$\begin{aligned} N^{00} &= \frac{v}{\sqrt{2}} \begin{pmatrix} e^{-iK_3} \cos K_2 & 0 \\ 0 & e^{iK_3} \cos K_1 \end{pmatrix} u \\ N^{01} &= \frac{v}{\sqrt{2}} \begin{pmatrix} 0 & -ie^{-iK_3} \sin K_2 \\ -ie^{iK_3} \sin K_1 & 0 \end{pmatrix} u \\ N^{10} &= \frac{v}{\sqrt{2}} \begin{pmatrix} 0 & -ie^{iK_3} \sin K_1 \\ -ie^{-iK_3} \sin K_2 & 0 \end{pmatrix} u \\ N^{11} &= \frac{v}{\sqrt{2}} \begin{pmatrix} e^{iK_3} \cos K_1 & 0 \\ 0 & e^{-iK_3} \cos K_2 \end{pmatrix} u, \end{aligned} \quad (214)$$

where $u, v \in SU(2)$ and $\vec{K} \in \mathbb{R}^3$.

These solvable states are quite useful. To see this and to give some intuition an example computation will be executed in the next section.

8.2 Time-Evolution of local Observables

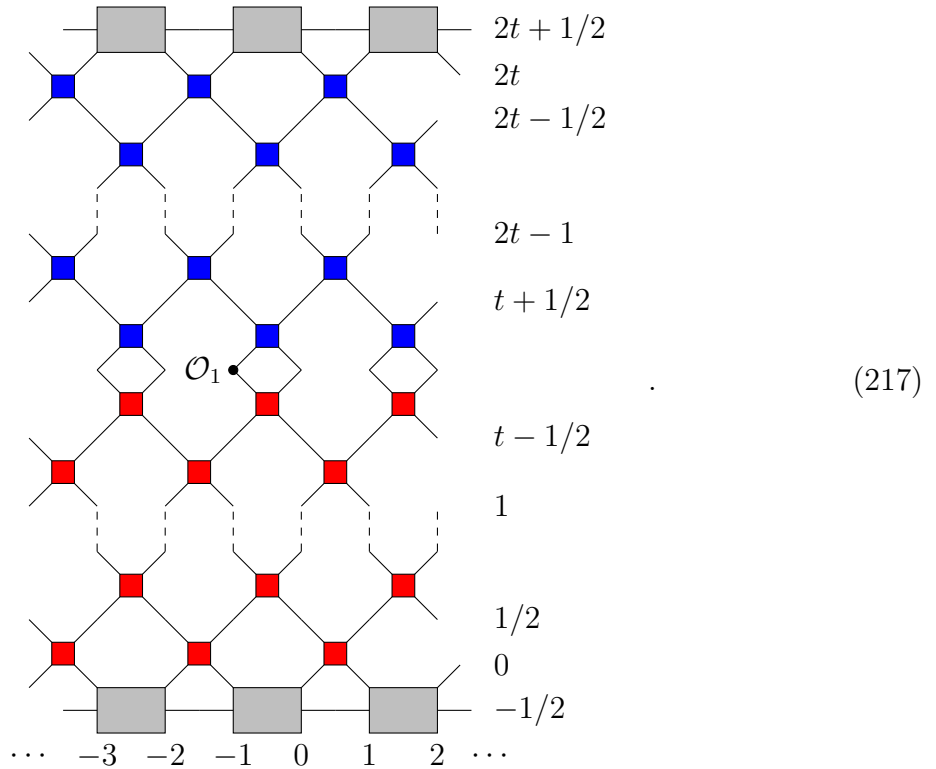
In this subsection we want to do a short computation to find

$$\lim_{L \rightarrow \infty} \langle \Psi_t^L | \mathcal{O}_1 | \Psi_t^L \rangle \quad , \quad (215)$$

where \mathcal{O}_1 is a local observable acting non-trivially only on a single site. Furthermore,

$$|\Psi_t^L\rangle = \mathbb{U}_L |\Psi_0^L\rangle \quad (216)$$

is the time evolved state, where \mathbb{U}_L is the usual time-evolution for a chain of length $2L$ as given in (16) with dual unitary operators U . However, we have to slightly change the enumeration scheme of our sites. The new scheme should be clear from the following visualisation of $\mathcal{O}_1 |\Psi_t^L\rangle$:



Rather than starting from an initial site 0 and increasing our count to the right, we start with sites -1 and 0 and increase the chain in length in both directions, using both positive and negative integers. With that scheme, we can now define a kind of transfer

operator

$$E_{\mathcal{O}_1}(t) = \begin{array}{c} \begin{array}{c} \text{---} \square \text{---} \\ \diagup \quad \diagdown \\ \square \quad \square \\ \diagdown \quad \diagup \\ \text{---} \end{array} & \begin{array}{l} 2t + 1/2 \\ 2t \\ 2t - 1/2 \end{array} \\ \vdots \\ \begin{array}{c} \text{---} \square \text{---} \\ \diagup \quad \diagdown \\ \square \quad \square \\ \diagdown \quad \diagup \\ \text{---} \end{array} & \begin{array}{l} 2t - 1 \\ t + 1/2 \end{array} \\ \mathcal{O}_1 \bullet & \\ \begin{array}{c} \text{---} \square \text{---} \\ \diagup \quad \diagdown \\ \square \quad \square \\ \diagdown \quad \diagup \\ \text{---} \end{array} & \begin{array}{l} t - 1/2 \\ 1 \end{array} \\ \vdots \\ \begin{array}{c} \text{---} \square \text{---} \\ \diagup \quad \diagdown \\ \square \quad \square \\ \diagdown \quad \diagup \\ \text{---} \end{array} & \begin{array}{l} 1/2 \\ 0 \\ -1/2 \end{array} \end{array} \quad (218)$$

We will write $E(t) = E_{\perp}(t)$. Using (211) and the dual unitary condition (23) it is easy to see that

$$|\mathcal{R}\rangle = \bigotimes_{\tau=1}^{t-1} \left(\frac{1}{\sqrt{d}} \sum_{j=1}^d |j\rangle_{\tau} \otimes |j\rangle_{2t+1-\tau} \right) \otimes \left(\frac{1}{\sqrt{\chi}} \sum_{j=1}^{\chi} |j\rangle_0 \otimes |j\rangle_{2t+1} \right) \quad (219)$$

is a right eigenvector of $E(t)$. Furthermore using (213) and (23) we find that

$$\langle \mathcal{L} | = (|\mathcal{R}\rangle)^{\dagger} \quad (220)$$

is a left eigenvector of $E(t)$. It was then argued in [6] that

$$\lim_{L \rightarrow \infty} \langle \Psi_t^L | \mathcal{O}_1 | \Psi_t^L \rangle = \langle \mathcal{L} | E_{\mathcal{O}_1}(t) | \mathcal{R} \rangle = \text{Tr}[\mathcal{O}_1]. \quad (221)$$

The last equation can be seen by using the above visualisation of $E_{\mathcal{O}_1}(t)$ and once more the relations (211) and (23). To be able to obtain exact results for an operators expectation value is very useful, we will expand on this example in the next section.

8.3 Implementation using Unitary Gates

In this section we will get even closer to application. To be more precise, we want to find a way to compute the quantity

$$\lim_{L \rightarrow \infty} \langle \Psi_t^L | \mathcal{O}_S | \Psi_t^L \rangle. \quad (222)$$

by running a quantum circuit on a quantum computer. The operator \mathcal{O}_S will be more general than the operator \mathcal{O}_1 in the previous section. We will start by establishing a tensor network that represents the quantity (222) as a tensor network in the next subsection.

8.3.1 Simplification of a Tensor Network

There is one immediate problem that comes to mind, when we want to establish a tensor numerically treatable tensor network for the quantity (222). The quantities computed in [6] were all in the limit $L \rightarrow \infty$. However, any realistic quantum computer will be finite. This in turn means that we can only hope to measure the properties of finitely extended operators. So we may restrict ourselves to the set of locally applied operators.

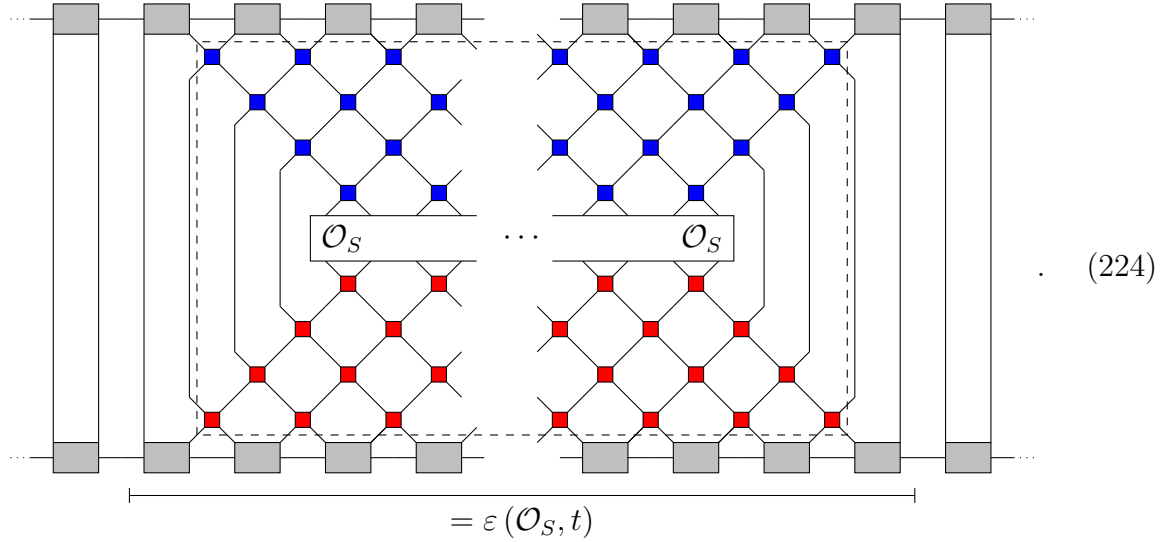
Def. 11. *An operator $\mathcal{O}_S \in \text{End}(\bigotimes_{i \in \mathbb{Z}} \mathcal{H}_i)$ with $S \subset \mathbb{Z}$ is called **locally applied** if there exist $a, b \in \mathbb{Z}$ such that $S \subset I_a(b)$ and \mathcal{O}_S acts trivially on sites outside of S .*

This restriction allows a proper implementation of (222), since we can now reduce the entire tensor network representing $\lim_{L \rightarrow \infty} \langle \Psi_t^L | \mathcal{O}_S | \Psi_t^L \rangle$ to a finite tensor network. We choose $a, b \in \mathbb{Z}$ with $S \subset I_a(b)$ such that a even, b odd and $|I_a(b)|$ minimal. We further limit the analysis to \mathcal{O}_S with $S = I_a(b)$. If S were not of such a form, we could extend \mathcal{O}_S to a locally applied operator $\mathcal{O}_{S'}$ with $S' = I_a(b)$ trivially by including the unit operators $\mathbb{1}$ that are applied on the site $S' \setminus S$. Now the notion of a light-cone $\mathcal{LC}(\mathcal{O}_S)$ extends easily to operators applied to multiple sites and the new enumerating system. Using a similar method to that established in section 4.2 one can find

$$\begin{aligned} \mathcal{LC}(\mathcal{O}_S) = & \\ \left\{ (z, \tau) \in \mathbb{Z} \times I_0(2t-1)/2 \mid \min_{z' \in \{a, b\}} |z - z'| \leq (2t-1) - 2\tau \right\} \cup & (I_a(b) \times I_0(2t-1)/2). \end{aligned} \tag{223}$$

This is the usual light-cone for the event (a, t) and (b, t) in union with all the events that have a space-coordinate $z \in S$ and a time-coordinate equal to or earlier than t . If we apply the unitary condition in time (22) for all operators not applied to an event in

$\mathcal{LC}(\mathcal{O}_S)$, the tensor network simplifies. For example for $t = 2$



Now we have an operator $\mathcal{O}_S(t)$, everything inside the dashed rectangle, that is locally applied to the set $I_{z_{\min}}(z_{\max})$, where

$$\begin{aligned} z_{\min} &= a - 2t + 1 \\ z_{\max} &= b + 2t - 1 \end{aligned} \quad (225)$$

are the minimal and maximal respectively space-coordinate that an event in \mathcal{LC} can have. On the left and right, we have infinitely long chains of the transfer operator T of N , which is defined as

$$T_{\alpha\beta}^{\tilde{\alpha}\tilde{\beta}} = \sum_{i,j=0}^{d-1} N_{\alpha\beta}^{ij} (N_{\tilde{\alpha}\tilde{\beta}}^{ij})^* \quad (226)$$

or via a tensor network diagram

$$T = \begin{array}{c} \text{---} N^* \text{---} \\ | \\ \text{---} N \text{---} \end{array} \quad (227)$$

The vector

$$|\mathcal{I}\rangle = \sum_{\beta=1}^{\chi} |\beta\rangle|\beta\rangle = \sum_{\beta,\tilde{\beta}=1}^{\chi} \delta_{\beta\tilde{\beta}} |\beta\rangle|\tilde{\beta}\rangle \quad (228)$$

is an unnormalised left- and right-eigenvector of T with eigenvalue 1. This follows immediately by applying the conditions (211) and (213) of N :

$$(T|\mathcal{I}\rangle)_{\alpha\tilde{\alpha}} = \sum_{i,j=0}^{d-1} N_{\alpha\beta}^{ij} (N_{\tilde{\alpha}\tilde{\beta}}^{ij})^* = \delta_{\alpha\tilde{\alpha}}. \quad (229)$$

As a tensor network this would be

$$\mathcal{I} \left[\begin{array}{c} N^* \\ N \end{array} \right] = \mathcal{I} \quad , \quad \left[\begin{array}{c} N^* \\ N \end{array} \right] \mathcal{I} = \mathcal{I} \cdot \quad (230)$$

Since we assumed $|\Psi^L\rangle$ to be normalised, 1 will be the eigenvalue with largest norm. For details refer to [6]. Thus we get

$$\lim_{L \rightarrow \infty} \langle \Psi_t^L | \mathcal{O}_S | \Psi_t^L \rangle = \lim_{L \rightarrow \infty} T^L \varepsilon(\mathcal{O}_S, t) T^L = \frac{1}{\chi} \langle \mathcal{I} | \varepsilon(\mathcal{O}_S, t) | \mathcal{I} \rangle. \quad (231)$$

Where does the factor $\frac{1}{\chi}$ come from? Since $|\mathcal{I}\rangle$ is not normalised, but $|\Psi^L\rangle$ is assumed to be normalised for all L , we get

$$1 = \lim_{L \rightarrow \infty} \langle \Psi_t^L | \mathbb{1} | \Psi_t^L \rangle \stackrel{!}{=} \nu \langle \mathcal{I} | \mathcal{I} \rangle = \nu \chi, \quad (232)$$

where $\nu \in \mathbb{R}$ is a constant. Therefore $\nu = \frac{1}{\chi}$. We will see the benefit in choosing $|\mathcal{I}\rangle$ to be unnormalised in the next subsection.

Equation (231) allows us to reduce our tensor network diagram (224) to the following finite form

$$\left[\begin{array}{c} \text{shaded box} \\ \text{shaded box} \\ \mathcal{O}_S(t) \\ \text{shaded box} \\ \text{shaded box} \end{array} \right] \cdots \left[\begin{array}{c} \text{shaded box} \\ \text{shaded box} \\ \mathcal{O}_S(t) \\ \text{shaded box} \\ \text{shaded box} \end{array} \right] \cdot \quad (233)$$

We can use this simplified tensor network diagram as a starting point to build an equivalent quantum circuit.

8.3.2 Conversion to a Quantum Circuit

A quantum circuit is a combination of quantum gates. All allowed gates have to be unitary operators along the time axis [28]. Therefore, we have to modify our tensor network to consist of only unitary matrices that are connected by normal matrix multiplication. While we did not specify the operator \mathcal{O}_S , we will assume that an implementation via unitary gates is known. The dual unitary gates are by definition easy to implement. So what remains are the N tensors. Their implementation is a little bit more involved, since we not only have the physical legs to worry about but also the virtual ones. While the physical indices fit easily into the circuit model of quantum computing, the virtual indices would flow perpendicular to the time direction in the quantum circuit. To overcome this problem, we will adapt a method used to implement MPS via unitary gates,

it is given in detail in [29]. A shorter explanation can be found in the appendix of [30]. In short, we want the tensors N to be included in a larger gate \mathbf{NG} . We will do this assuming we have access to qudits, i.e. systems that have a d -dimensional Hilbert space. This is the same dimension as for our physical legs. Ways to realise qudit systems and how to work with them exist, e.g. cf. [31], so this is a reasonable assumption.

We need two qudits to account for the physical legs and $n = \lceil \log_d \chi \rceil$ -many qudits to act on a big enough state space to include the vertical legs. Therefore let \mathbf{NG} be a gate acting on $2 + \lceil \log_d \chi \rceil$ qudits. The elements of such a gate \mathbf{NG} can be represented as

$$\begin{array}{c}
 |i\rangle \quad |j\rangle \quad |\beta_1\rangle \quad \dots \quad |\beta_{n-2}\rangle \quad |\beta_{n-1}\rangle \quad |\beta_n\rangle \\
 \hline
 \mathbf{NG} \quad \dots \quad \mathbf{NG} \\
 \hline
 |\alpha_1\rangle \quad |\alpha_2\rangle \quad |\alpha_3\rangle \quad \dots \quad |\alpha_n\rangle \quad |p_1\rangle \quad |p_2\rangle
 \end{array} , \quad (234)$$

where all the indices take values in $I_0(d-1)$. We define some of these matrix-elements via

$$\langle i, j, \beta_1 \dots \beta_n | \mathbf{NG} | \alpha_1 \dots \alpha_n, 0, 0 \rangle = N_{\alpha\beta}^{ij} \quad \text{for } \alpha, \beta \in I_0(\chi-1), \quad (235)$$

where $\alpha_1 \dots \alpha_n$ is the representation of $\alpha-1$ in the numeral system with base d , same for β . We will from here on write α instead of the full $\alpha_1 \dots \alpha_n$, again the same for β . Thus the gate visualisation simplifies to

$$\begin{array}{c}
 |i\rangle \quad |j\rangle \quad |\beta\rangle \\
 \hline
 \mathbf{NG} \\
 \hline
 |\alpha\rangle \quad |p_1\rangle \quad |p_2\rangle
 \end{array} . \quad (236)$$

To get precisely the matrix elements corresponding to the tensor N , we will only need to ensure the $|p_k\rangle$ are prepared in the $|0\rangle$ state. If $\chi < d^n$, the matrix elements with $|p_1, p_2\rangle = |0, 0\rangle$ and $\beta > \chi - 1$ are not yet defined. We can just set them as 0. Thus, the column vectors $\mathbf{NG}|\alpha, 0, 0\rangle$ are defined, but only for $\alpha \in I_0(\chi-1)$. These have to be orthonormal for \mathbf{NG} to be unitary. Condition (211) provides exactly that orthonormality:

$$\langle \alpha, 0, 0 | \mathbf{NG}^\dagger \mathbf{NG} | \tilde{\alpha}, 0, 0 \rangle = \sum_{ij\beta} N_{\alpha\beta}^{ij} (N_{\tilde{\alpha}\beta}^{ij})^* = \delta_{\tilde{\alpha}\alpha}. \quad (237)$$

The partial trace is most certainly a valid quantum operation [34] or superoperator [35]. However, it is not part of the traditional model of quantum computing [35], i.e. the circuit model. This means we cannot realise it just using a unitary gate with the number qudits we have in $\mathbf{circ}_{\text{init}}$. Luckily, there is another way. We repeat the method, used before to get \mathbf{NG} , but now with a gate \mathbf{LNG} acting on $\lceil \log_d \chi \rceil$ additional qubits:

$$\begin{array}{cccc}
 |\alpha\rangle & |i\rangle & |j\rangle & |\beta\rangle \\
 \hline
 & \mathbf{LNG} & & \\
 \hline
 |p_1\rangle & |p_2\rangle & |p_3\rangle & |p_4\rangle
 \end{array} . \quad (240)$$

As before we shortened all the qudits making up $|\alpha\rangle$ and $|\beta\rangle$ into a single symbol. This time we define some of the matrix elements as

$$\langle \alpha, i, j, \beta | \mathbf{LNG} | 0, 0, 0, 0 \rangle = \frac{1}{\sqrt{\chi}} N_{\alpha\beta}^{ij}. \quad (241)$$

We can find the remaining matrix elements the same as before: We complete the column vectors partially defined by the equation (241) with zeros and find the remaining column vectors using the fact that \mathbf{LNG} should be unitary. But why does an additional factor pop up at this point?

Again the column vectors need to be orthonormal for \mathbf{LNG} to be unitary. However, this time we sum over an additional leg. Using (211) we get

$$1 = \langle 0, 0, 0, 0 | \mathbf{LNG}^\dagger \mathbf{LNG} | 0, 0, 0, 0 \rangle \stackrel{!}{=} \nu^2 \sum_{\alpha ij\beta} N_{\alpha\beta}^{ij} (N_{\alpha\beta}^{ij})^* = \nu^2 \chi. \quad (242)$$

Thus the additional factor $\nu = \frac{1}{\sqrt{\chi}}$ is justified. Our new circuit is then

$\text{circ} =$

 $|0\rangle |0\rangle |0\rangle |0\rangle |0\rangle |0\rangle |0\rangle |0\rangle$
 LNG^\dagger

 LNG
 $|0\rangle |0\rangle |0\rangle |0\rangle |0\rangle |0\rangle |0\rangle |0\rangle$

 \dots

 $|0\rangle |0\rangle |0\rangle |0\rangle |0\rangle |0\rangle$

 $|0\rangle |0\rangle |0\rangle |0\rangle |0\rangle |0\rangle$

 $, \quad (243)$

which can be run on a circuit based quantum computer, such as provided by IBM in the form of Qiskit and the IBM-Quantum Lab [36]. It also fulfils the desired equation

$$\lim_{L \rightarrow \infty} \langle \Psi_t^L | \mathcal{O}_S | \Psi_t^L \rangle = \langle 0, \dots, 0 | \text{circ} | 0, \dots, 0 \rangle. \quad (244)$$

We can run the circuit multiple times and measure. By doing so we find the overlap of the final state $\text{circ}|0, \dots, 0\rangle$ with $|0, \dots, 0\rangle$, which is exactly the quantity that calculates the original tensor network, as shown by (244).

As a sidenote, we assumed \mathcal{O}_S to also be a unitary. However, general physical quantities are given by hermitian operators. Measuring those is possible using an appropriate quantum simulator as defined in [37]. We would only need to run the first half of our circuit, i.e. up to the application of \mathcal{O}_S . At this point the simulator's state would be

equivalent to the state after the time-evolution. Rather than running \mathcal{O}_S as a gate, one can now measure it directly and obtain the desired physical quantity that way. Note that only the conventional unitary condition in time direction was used to get to our end result. However, the important difference between general unitary gates and dual unitary gates is that for the latter we know an easy and exact solution. Therefore we can check our results against the exact solution. This could allow us to get benchmark solutions for quantum computers as well as classical computations for the contraction of such a tensor network. The results coming from both could show, if quantum computers have an advantage in calculating such dynamics and thus if they may be used to compute dynamics using general unitary gates. This is even more useful for a system with more spatial dimensions.

8.4 Solvable States for two spatial Dimensions

What we did with a solvable MPS on a one-dimensional chain of systems lead to an interesting application. Two-dimensional quantum lattices are even harder to handle both analytically [13] as well as numerically [5]. In section 5 we already extended the concept of dual unitaries, which were incremental for the success in the previous subsections on solvable states, to two spatial dimensions. Thus it seems reasonable to extend the solvable states to two space-dimensions. Note that this section is not perfectly worked out and lacks some of the precision the other sections had, since this is still part of ongoing research.

There already exists a class of states on a 2D-lattice that would correspond to the MPS, the so called projected entangled pair states (PEPS) [10]. For such a state, each individual system is described by a 5-tensor, with four virtual bonds to the four nearest neighbours and one physical bond. A 2D lattice state $|\Psi^{L_1, L_2}\rangle$ for a lattice of size $2L_1 \times 2L_2$ in PEPS-form can be represented using a tensor network diagram

$$|\Psi^{L_1, L_2}\rangle = \text{Diagram of a 2D lattice of tensors with red legs and axes } e_1, e_2, \quad (245)$$

where the red legs represent the physical bonds and we assume periodic boundary conditions. Note that the lattice does not need to be a square and we can choose $L_1 \neq L_2$ just as well. Similar to the MPS-chain, we want the PEPS to be two-site shift-invariant, but this time in both spatial dimensions. Therefore we combine the four tensors describing a plaquette of systems into a single tensor:

$$N = \text{Diagram of a 2x2 plaquette of tensors} = \text{Diagram of a single shaded tensor } N, \quad (246)$$

Thus N is a 12-tensor. Again, even though we used a symmetric symbol for N , that does not mean it is symmetric under rotation by multiples of $\frac{\pi}{2}$.

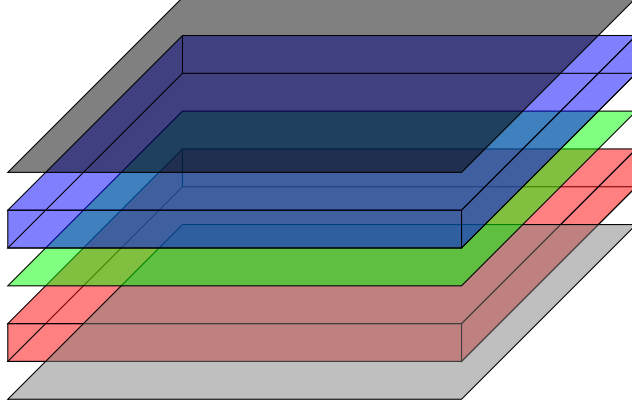


Figure 9: This is a sketch of the tensor network diagram of the quantity $\langle \Psi^{L_1, L_2}(t) | \mathcal{O}_S | \Psi^{L_1, L_2}(t) \rangle$, therefore no tensor legs are included. We will go from bottom to top. The gray square at the bottom represents $|\Psi^{L_1, L_2}(0)\rangle$, which is made up of plaquette tensors N . Next comes the red box which corresponds to the time-evolution \mathbb{U}^t . Somewhere inside the green layer \mathcal{O}_S is applied. The blue box represents $(\mathbb{U}^\dagger)^t$. Finally the top black square represents $|\Psi^{L_1, L_2}(0)\rangle$ consisting of the plaquette tensors N^* .

Furthermore, we will assume that parallel legs have the same dimension. We will denote the dimension of the virtual bonds parallel to direction e_1 and e_2 respectively by χ_1, χ_2 . The physical dimension is as usual denoted by d . $|\Psi^{L_1, L_2}(N)\rangle$ will then consist of the same plaquette tensor N for each plaquette instead of a potentially different 12-tensor at each plaquette. Usually we will leave the N out of the state expression.

We are now ready to apply a time-evolution to any state, for example the evolution \mathbb{U} consisting of our ternary unitaries as given in (87). The precise application of the unitaries relative to the plaquettes is important for exact computations, but will not concern us right now. As before we will assume that $|\Psi^{L_1, L_2}(t)\rangle = \mathbb{U}^t |\Psi^{L_1, L_2}(0)\rangle$ is normalised for all L_1, L_2 and times t . This time we want to find the quantity

$$\overline{\mathcal{O}_S} = \lim_{L_2 \rightarrow \infty} \lim_{L_1 \rightarrow \infty} \overline{\mathcal{O}_S}(L_1, L_2, t) = \lim_{L_2 \rightarrow \infty} \lim_{L_1 \rightarrow \infty} \langle \Psi^{L_1, L_2}(t) | \mathcal{O}_S | \Psi^{L_1, L_2}(t) \rangle, \quad (247)$$

where \mathcal{O}_S an operator applied to the sites in S . We will see later on that the order of the limits is important. Due to the same reasoning as before, we restrict ourselves to locally applied \mathcal{O}_S . For finite L_1, L_2 the tensor network diagram associated to $\overline{\mathcal{O}_S}(L_1, L_2)$ looks like a sandwich. A sketch of it is given in Fig. 9.

We once more need to reduce the infinite tensor network representing $\overline{\mathcal{O}_S}$ to a finite one to compute (247). Since we assumed \mathcal{O}_S to be locally applied, we may once more use the light-cone method already used in sections 4.2, 5.2, 6 and to get (223). Just as in the 1D-case, all unitary operators in the time-evolution \mathbb{U}^t will reduce to the identity, except for those applied to events in a finite set. As before, we may combine both the operator \mathcal{O}_S and what remains of the time-evolution into a new operator $\mathcal{O}_S(t)$. This new operator will be locally applied on a rectangular set $\tilde{S} = I_{x_{\min}}(x_{\max}) \times I_{y_{\min}}(y_{\max}) \supset S$. We may

write

$$\overline{\mathcal{O}_S}(t) = \lim_{L_2 \rightarrow \infty} \lim_{L_1 \rightarrow \infty} \langle \Psi^{L_1, L_2}(0) | \mathcal{O}_S(t) | \Psi^{L_1, L_2}(0) \rangle. \quad (248)$$

To continue, we have to define what a solvable state actually is in two spatial dimensions. We will have to define desired properties separately for each dimension.

Def. 12. A class of two-site shift-invariant PEPSs $\{|\Psi^{L_1, L_2}(N)\rangle\}_{L_1, L_2}$ defined by plaquette 12-tensors N is called **periodically solvable** in direction e_i if a chain $C_i(L, N)$ of L -many N -tensors along direction e_j (with $j \neq i$) fulfils

$$= \frac{1}{d^2} \quad (249)$$

for all L and for periodic boundary conditions on the chain's ends.

We will assume our class of sets to be periodically solvable in e_1 -direction. We can then define a kind of transfer operator

$$T = \quad (250)$$

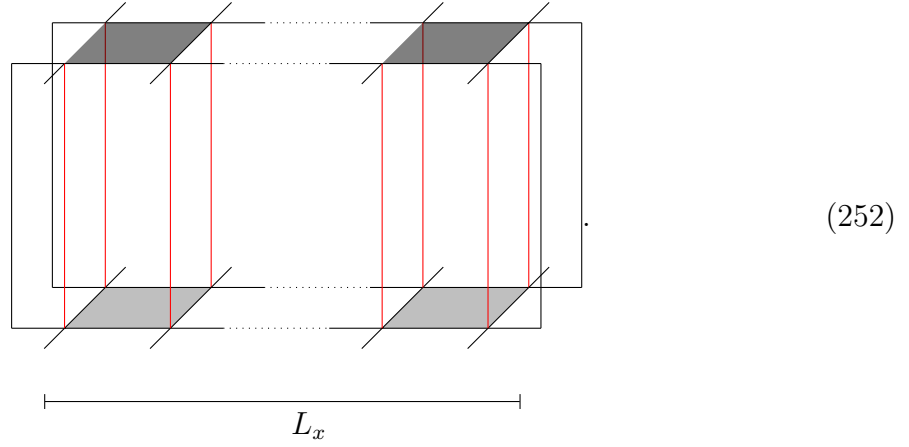
For any plaquettes describing systems outside of \tilde{S} , only this transfer operator will be left. Specifically for the plaquette operators defined on a plaquette $p(x, y)$ with $x \notin I_{x_{\min}}(x_{\max})$, we will have an infinite chain of transfer operators along the e_2 direction. The solvability condition (249) and normalisation of our PEPS imply that $C_1(L, N)$ has a maximum eigenvalue 1 with eigenvector $|\mathcal{I}\rangle^{\otimes 2L}$, where $|\mathcal{I}\rangle$ is defined as in equation (229). Thus using the same argumentation as in the 1D-case, we can reduce our tensor network to a finite tensor network in e_1 -direction

$$\overline{\mathcal{O}_S}(t) = \lim_{L_2 \rightarrow \infty} \langle \mathcal{I} |^{\otimes 2L_x} (\langle \Psi^{L_x, L_2}(0) | \mathcal{O}_S(t) | \Psi^{L_x, L_2}(0) \rangle) | \mathcal{I} \rangle^{\otimes 2L_x}, \quad (251)$$

where $L_x > x_{\max} - x_{\min}$ is finite, but large enough to contain \tilde{S} .

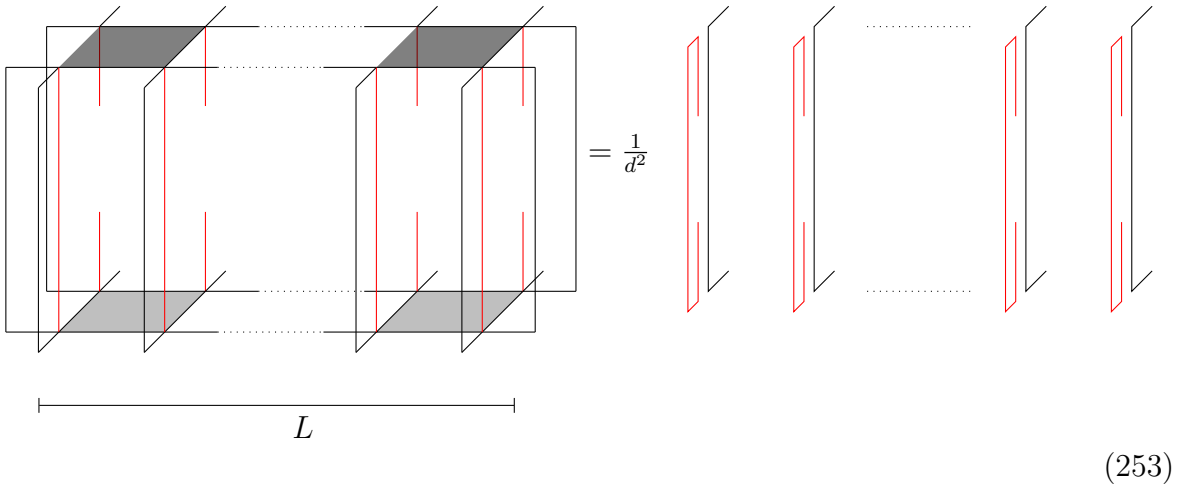
However, the network still extends infinitely in the e_2 -direction. Simply demanding (249)

again will not help, since the boundary conditions of the chains of L_x -many tensors N along direction e_1 are not periodic but rather $|\mathcal{I}\rangle^{\otimes 2}$. Visually get for a chain $C_2(L_x, N)$ outside of \tilde{S} the following:



Thus we have a chain of L_x -many transfer operators T for every $y \notin I_{y_{\min}}(y_{\max})$. So we may define

Def. 13. A class of two-site shift-invariant PEPSs $\{|\Psi^{L_1, L_2}(N)\rangle\}_{L_1, L_2}$ defined by plaquette 12-tensors N is called $|\mathcal{I}\rangle^{\otimes 2}$ -**solvable** in direction e_i if a chain $C_i(L, N)$ of L -many N -tensors along direction e_j (with $j \neq i$) fulfils



for all L .

By assuming that our class of states is $|\mathcal{I}\rangle^{\otimes 2}$ -solvable as well and using an analogous argument as to get equation (251), we can also reduce our tensor network in e_2 direction to a finite size.

$$\overline{\mathcal{O}_S(t)} = \langle \mathcal{I} |^{\otimes 4L_x L_y} \left(\langle \Psi^{L_x, L_y}(0) | \mathcal{O}_S(t) | \Psi^{L_x, L_y}(0) \rangle \right) | \mathcal{I} \rangle^{\otimes 4L_x L_y}, \quad (254)$$

where $L_y > y_{\max} - y_{\min}$. Thus we again managed to get a finite tensor network representing the desired quantity.

However, there are two things to note. The arguments to reduce the tensor network's size only required that $|\mathcal{I}\rangle^{\otimes 2}$ is an eigenvector of T with eigenvalue 1 for every direction. What we demanded is stronger, so the result (254) will hold already if we only demand that T has an eigenvector with eigenvalue 1. However, in analogy to the 1D-case, our assumptions will allow for an exact solution to be computed. Secondly, note that this process is not symmetric under exchange of directions $e_1 \leftrightarrow e_2$ and thus the limits in the initial expression for $\overline{O}_S(t)$ clearly cannot be commuted. We can allow for this by making even more assumptions, either by demanding our class of states to be both periodically solvable and $|\mathcal{I}\rangle^{\otimes 2}$ -solvable in both directions or by making generalising our assumptions for state class $|\Psi^{L_1, L_2}\rangle$ to all boundary conditions. But clearly these are even stricter conditions and might be too much to still find a class of states. The undertaking of finding example states is already hard, except for a simple one:

Example 6. *We just assume $\chi_2 = 1$. We can also set the bound dimension in e_2 -direction inside of N to one. Hence*

$$N = \text{[Diagram 1]} = \text{[Diagram 2]} . \quad (255)$$

By demanding the resulting 4-tensors to have the same properties as the 4-tensors making up the solvable states in one-spatial dimension, we get precisely what was demanded of N in the definitions 12 and 13. This example might be considered quite trivial since it solves the problem of different boundary conditions by just discarding one direction.

In analogy to the case of one-spatial dimension in section 8.3.2, one can try to rework the finite tensor network into a quantum circuit using mostly the same tricks. Furthermore, it will be useful to assume the existence of a two-dimensional quantum computer to implement this more easily. This is not an unreasonable assumption, cf. [38]. A more detailed exploration of these kinds of states is still in the making. Especially finding more examples will turn out to be useful in order to actually use them in a benchmarking method for two-dimensional quantum computers. However, on the analytical side the exact solutions still need to be worked out precisely to do this. Still, intuitively it seems clear that those exist.

With this done we arrived where we initially hoped to end up. So let us wrap everything up.

9 Final Discussion and Outlook

Our journey is almost at the end. First let us recapitulate what we found. We discussed the concept of dual unitary operators and extended it to two spatial dimensions

by defining ternary unitary operators, for which we found examples in the form of the constructions X and Y given in equations (77) and (78) respectively. We generalised the idea even further to arbitrary dimensions by defining $(\Delta + 1)$ -unitary operators. By using the methods and language developed in $(1 + 1)$ -dimensional space-time and abstracting that in $(2 + 1)$ -dimensional space-time using visual aid, we managed to even find exact results for the correlation function $D^{\alpha\beta}(x, y, t)$ after arbitrary times for $(\Delta + 1)$ -dimensional space-time. We explored these results further by introducing and analysing the M -maps. Then we had a quick look at the more fundamental origins of the different classes of unitaries, some of which are examples of $(\Delta + 1)$ -unitaries. A quick overview of the current connections made between them in the literature was given as well. In the final section we returned to lower dimensions, where we found a benchmarking possibility for quantum computers. We did so successfully by utilising the concept of unitary states and manipulation of tensor networks in order to get a usable finite quantum circuit that can be run on a quantum computer. While we completed this task for one spatial dimension, we gave only a general plan for the more difficult two-dimensional problem.

Thus we found quite a lot of nice results during this journey. However, more research pathways were opened up and questions left unanswered, so one might consider this end merely a pause. Further exploration and analysis on the topic of $(\Delta + 1)$ -unitaries could include the two subsets of $\mathcal{TU}(d)$ that were given in (77) and (78). Do they describe the entire set of ternary unitaries or merely a subset and can we find a complete parametrisation of $\mathcal{TU}(d)$? One may use a numerical method similar to the one used in the estimations in [39] to get an idea of the real parameters required. Or one could start right away from various general parametrisations of unitary matrices [40,41]. This might also pave the way to a general parametrisation of $(\Delta + 1)$ -unitaries.

A different direction one could take is to extend other properties and settings of dual unitaries that have been analysed in the literature to higher dimensions, each of which might give rise to an entire thesis on its own. Examples include a folding of gates to combine an operator with its hermitian conjugate, to allow for easier computations, the analysis of operator entanglement [2], entanglement barriers [42] and the behaviour under perturbation by non-dual-unitary operators [4].

Finally, note that we did not run our quantum circuit `circ` as given in equation (243) on an actual quantum computer. At the same time one should try to contract the tensor network in equation (233) on a classical computer and compute the exact result for some example of dual unitaries and solvable states, examples for the latter are given in [6]. All of this still provides plenty to explore especially in two spatial dimensions. Although we have arrived at our initial goal, we can see multiple new pathways opening up for future research.

References

- [1] Bertini B, Kos P, Prosen T. 2019 Exact correlation functions for dual-unitary lattice models in 1+1 dimensions. *Physical Review Letters* **123**, 210601. (doi:10.1007/BF01328601).
- [2] Bertini B, Kos P, Prosen T. 2020 Operator entanglement in local quantum circuits i: Chaotic dual-unitary circuits. *SciPost Phys.* **8**, 67. (doi:10.21468/SciPostPhys.8.4.067).
- [3] Jonay C, Khemani V, Ippoliti M. 2021 Tri-unitary quantum circuits. *Physical Review Research* **3**, 4. (doi:10.1103/physrevresearch.3.043046).
- [4] Kos P, Bertini B, Prosen T. 2021 Correlations in perturbed dual-unitary circuits: Efficient path-integral formula. *Phys. Rev. X* **11**, 011022. (doi:10.1103/PhysRevX.11.011022).
- [5] Orús R. 2019 Tensor networks for complex quantum systems. *Nature Reviews Physics* **1**, 9, 538–550. (doi:10.1038/s42254-019-0086-7).
- [6] Piroli L, Bertini B, Cirac JI, Prosen T. 2020 Exact dynamics in dual-unitary quantum circuits. *Phys. Rev. B* **101**, 094304. (doi:10.1103/PhysRevB.101.094304).
- [7] Nolting W. 2013 *Quantenmechanik - Grundlagen*, vol. 5,1 of *Grundkurs theoretische Physik*. Springer, 8. ed.
- [8] Schollwöck U. 2011 The density-matrix renormalization group in the age of matrix product states. *Annals of Physics* **326**, 1, 96–192. (doi:10.1016/j.aop.2010.09.012).
- [9] Nolting W. 2015 *Viel-Teilchen-Theorie*, vol. 7 of *Grundkurs theoretische Physik*, chap. 2.4.2, pp. 88–91. Springer, 8 ed.
- [10] Orús R. 2014 A practical introduction to tensor networks: Matrix product states and projected entangled pair states. *Annals of Physics* **349**, 117–158. (doi:10.1016/j.aop.2014.06.013).
- [11] Faddeev LD. 1996. How algebraic bethe ansatz works for integrable model.
- [12] M Reed BS. 1980 *Functional Analysis*, vol. I of *Methods of Modern Mathematical Physics*, chap. VI: Bounded Operators. Academic Press, revised and enlarged edition ed.
- [13] Suzuki R, Mitarai K, Fujii K. 2021 Computational power of one- and two-dimensional dual-unitary quantum circuits .
- [14] Gross R, Marx A. 2018 *Festkörperphysik*. De Gruyter. (doi:10.1515/9783110559187).
- [15] Price HM. 2020 Four-dimensional topological lattices through connectivity. *Physical Review B* **101**, 20. (doi:10.1103/physrevb.101.205141).

- [16] Kendall MG. 1961 *A course in the Geometry of n Dimensions*, vol. 8 of *Griffin's Statistical Monographs & Courses*. Charles Griffin & CO. LTD.
- [17] Musz M, Kuś M, Życzkowski K. 2013 Unitary quantum gates, perfect entanglers, and unistochastic maps. *Physical Review A* **87**, 2. (doi:10.1103/physreva.87.022111).
- [18] Bengtsson I, Życzkowski K. 2006 *Quantum operations*, p. 251–280. Cambridge University Press. (doi:10.1017/CBO9780511535048.011).
- [19] Choi MD. 1975 Completely positive linear maps on complex matrices. *Linear Algebra and its Applications* **10**, 3, 285–290. (doi:10.1016/0024-3795(75)90075-0).
- [20] Higham NJ. 2008 *Functions of Matrices: Theory and Computation*, chap. 1: Theory of Matrix Functions, pp. 1–34. SIAM. (doi:10.1137/1.9780898717778).
- [21] Vidal G. 2007 Classical simulation of infinite-size quantum lattice systems in one spatial dimension. *Physical Review Letters* **98**, 7. (doi:10.1103/physrevlett.98.070201).
- [22] Gu ZC, Levin M, Wen XG. 2008 Tensor-entanglement renormalization group approach as a unified method for symmetry breaking and topological phase transitions. *Physical Review B* **78**, 20. (doi:10.1103/physrevb.78.205116).
- [23] Jiang HC, Weng ZY, Xiang T. 2008 Accurate determination of tensor network state of quantum lattice models in two dimensions. *Physical Review Letters* **101**, 9. (doi:10.1103/physrevlett.101.090603).
- [24] Pastawski F, Yoshida B, Harlow D, Preskill J. 2015 Holographic quantum error-correcting codes: toy models for the bulk/boundary correspondence. *Journal of High Energy Physics* **2015**, 6. (doi:10.1007/jhep06(2015)149).
- [25] Harris RJ, McMahon NA, Brennen GK, Stace TM. 2018 Calderbank-shor-steane holographic quantum error-correcting codes. *Physical Review A* **98**, 5. (doi:10.1103/physreva.98.052301).
- [26] Goyeneche D, Alsina D, Latorre JI, Riera A, Życzkowski K. 2015 Absolutely maximally entangled states, combinatorial designs, and multiunitary matrices. *Physical Review A* **92**, 3. (doi:10.1103/physreva.92.032316).
- [27] Perez-Garcia D, Verstraete F, Wolf MM, Cirac JI. 2007 Matrix product state representations. *Quantum Info. Comput.* **7**, 5, 401–430. (doi:10.26421/QIC7.5-6-1).
- [28] Nielsen MA, Chuang IL. 2010 *Quantum Computation and Quantum Information*, chap. II.4 Quantum Circuits, pp. 171–215. Cambridge University Press, 10th anniversary ed.

- [29] Barratt F, Dborin J, Bal M, Stojevic V, Pollmann F, Green AG. 2021 Parallel quantum simulation of large systems on small nisq computers. *npj Quantum Information* **7**, 1. (doi:10.1038/s41534-021-00420-3).
- [30] Lin S, Dilip R, Green AG, Smith A, Pollmann F. 2021 Real- and imaginary-time evolution with compressed quantum circuits. *PRX Quantum* **2**, 010342. (doi:10.1103/PRXQuantum.2.010342).
- [31] Wang Y, Hu Z, Sanders BC, Kais S. 2020 Qudits and high-dimensional quantum computing. *Frontiers in Physics* **8**. (doi:10.3389/fphy.2020.589504).
- [32] Knabner P, Barth W. 2013 *Lineare Algebra*, chap. 4.6 Die Singulärwertzerlegung. Springer. (doi:10.1007/9783642321863).
- [33] Milbradt R. 2021. <https://github.com/Drachier/GateCreationforSolvableStates>.
- [34] Nielsen MA, Chuang IL. 2010 *Quantum Computation and Quantum Information*, chap. III.8.3 Examples of quantum noise and quantum operations, pp. 373,374. Cambridge University Press, 10th anniversary ed.
- [35] Vizzotto J, Altenkirch T, Sabry A. 2006 Structuring quantum effects: superoperators as arrows. *Mathematical Structures in Computer Science* **16**, 3, 453–468. (doi:10.1017/S0960129506005287).
- [36] Asfaw A, Corcoles A, Bello L, Ben-Haim Y, Bozzo-Rey M, Bravyi S, Bronn N, Capelluto L, Vazquez AC, Ceroni J, *et al.* 2020 *Learn Quantum Computation Using Qiskit*.
- [37] Johnson T, Clark S, Jaksch D. 2014 What is a quantum simulator? *EPJ Quantum Technology* **1**, 10. (doi:10.1140/epjqt10).
- [38] Liu X, Hersam M. 2019 2d materials for quantum information science. *Nature Reviews Materials* **4**, 669–684. (doi:10.1038/s41578-019-0136-x).
- [39] Prosen T. 2021 Many-body quantum chaos and dual-unitarity round-a-face. *Chaos: An Interdisciplinary Journal of Nonlinear Science* **31**, 9, 093101. (doi:10.1063/5.0056970).
- [40] Spengler C, Huber M, Hiesmayr BC. 2010 A composite parameterization of unitary groups, density matrices and subspaces. *Journal of Physics A: Mathematical and Theoretical* **43**, 38, 385306. (doi:10.1088/1751-8113/43/38/385306).
- [41] Dita P. 1982 Parametrisation of unitary matrices. *Journal of Physics A: Mathematical and General* **15**, 11, 3465–3473. (doi:10.1088/0305-4470/15/11/023).
- [42] Reid I, Bertini B. 2021 Entanglement barriers in dual-unitary circuits. *Physical Review B* **104**, 1. (doi:10.1103/physrevb.104.014301).